

## 2.4S.6 Probable Maximum Tsunami Hazards

This subsection examines the Probable Maximum Tsunami (PMT) at the STP 3 & 4 site.

Evaluation of the PMT, as defined by Reference 2.4S.6-1, requires the use of best available scientific information to arrive at a set of scenarios reasonably expected to affect a nuclear power plant site. Reference 2.4S.6-1 recommends a hierarchical hazard assessment for screening exposure to hazards from natural phenomena. The hierarchical screening process is based on a series of stepwise, progressively more refined analyses that evaluate hazards resulting from a tsunami. The hierarchical hazard assessment includes regional screening, site screening, and, if necessary, a detailed PMT hazard assessment.

For this subsection, a tsunami may be characterized as a solitary positive wave, a negative wave coupled with a positive wave (i.e., an N-wave), a series of waves, or any combination of wave types with parameters defined by Table 2.4S.6-1 and Table 2.4S.6-2.

The STP 3 & 4 site is located about 15 mi (24 km) from the South Texas coast (Figure 2.4S.6-1). The site is about 3.2 mi west of the Lower Colorado River, and about 17 river miles, as measured in plan view along the Lower Colorado River, from the South Texas coast. The site grade elevations in the STP 3 & 4 power block area range from 32 ft MSL to 36.6 ft MSL, and all safety-related facilities in the power block are designed to be water tight at or below elevation 40.0 ft MSL as discussed in Subsection 2.4S.10. In addition, the Ultimate Heat Sink (UHS) and Pump House are designed to be watertight below 50 ft MSL (Subsection 2.4S.2.2). Flooding from tsunami events is not expected to affect the safety functions of the plant as discussed below.

### 2.4S.6.1 Probable Maximum Tsunami

Tsunamis are gravity waves generated by large underwater disturbances. Reference 2.4S.6-1, Reference 2.4S.6-2, and Reference 2.4S.6-3 identify several types of tsunamigenic source mechanisms, including seismic events, volcanic events, submarine mass failures (SMFs), subaerial landslides, and impact of projectiles. With respect to a tsunami hazard assessment for the STP 3 & 4 project site, three primary forcing mechanisms are included in the analysis: seismic events, volcanic events, and SMFs (Reference 2.4S.6-1).

The tsunami hazard on the Gulf coast is summarized in Reference 2.4S.6-3. With respect to seismic events, Reference 2.4S.6-3 states that "tsunamis generated by earthquakes do not appear to impact the Gulf of Mexico coast." Further, simulations of postulated "worst-case" far-field (i.e., tsunami sources originating from over 1000 km away) seismic events with potential to affect the US Gulf coast indicate a maximum wave height of about 0.15 m at the South Texas coast (Reference 2.4S.6-4). With respect to volcanic events, the largest conjectured event with potential to affect the US Atlantic and Gulf coasts has been postulated to be a tsunami from the eruption and collapse of the Cumbre Vieja volcano on the island of La Palma in the Canary Islands

(Reference 2.4S.6-5). However, Reference 2.4S.6-3 indicates that this event is unlikely to affect the Gulf coast.

With respect to SMFs, Reference 2.4S.6-3 identifies several large SMF scars in carbonate, salt, and canyon to deep-sea provinces in the Gulf of Mexico. Many scars in these provinces correspond with relic events throughout the Quaternary (i.e., from 2.6 million to about 7500 years before the present, or yr BP). Multiple events have been identified for each scar. Notably, the geomorphology of SMFs in the Gulf of Mexico has been shown to be coupled with changes in sea level (Reference 2.4S.6-6 and Reference 2.4S.6-7). Reference 2.4S.6-6 documents sea-level changes over the last 140,000 years, with the last lowstand of 120 m below present sea level occurring less than 20,000 years ago.

With respect to near-field tsunami hazards at STP 3 & 4 (i.e., tsunamigenic sources within 124 mi or 200 km), the most prominent SMF scar is the East Breaks slump. The East Breaks slump is located approximately 88.2 mi (142 km) to the southeast of STP 3 & 4. Characterization and analysis of the East Breaks slump are discussed in detail in Subsection 2.4S.6.4.

Based on the hierarchical hazard assessment, the PMT for the STP 3 & 4 site is conjectured to occur from an SMF similar to the East Breaks slump. However, as the interpretation of a single wave height from a slump scar may not be sufficient to bound the PMT flood risks on STP 3 & 4 due to the uncertainties inherent in the assessment, a range of potential conditions were simulated at the East Breaks slump location. Simulations were performed using a hydrodynamic code known as the Method of Splitting Tsunami (MOST) (References 2.4S.6- 8 and 2.4S.6-9). These simulations were intended to bracket any near-field tsunami hazard from a SMF in the Gulf of Mexico.

Initial conditions of a negative wave (i.e., a wave caused by the drawdown of the water surface due to a sliding mass) were based on curve fits of sliding block experiments of Reference 2.4S.6-10 and Reference 2.4S.6-11. These initial conditions were subsequently scaled into a three-dimensional dipole wave (i.e., a negative wave and positive wave with unequal intensities) based on relationships presented in References 2.4S.6-12, 2.4S.6-13, and 2.4S.6-14.

The SMF scenarios postulated include initial wave deformation areas (i.e., areas differing from MSL) ranging from 410 km<sup>2</sup> to 9932 km<sup>2</sup> (158 mi<sup>2</sup> to 3835 mi<sup>2</sup>, respectively). Four scenarios were modeled as candidate PMT events. The simulation results indicate that all candidate PMT events were rapidly diffused by the continental shelf offshore of the South Texas coast, with nearly all remaining wave energy being reflected by the barrier islands. For negative wave elevations ranging from -7 m (23.0 ft) to -140 m (459.3 ft) and positive wave elevations ranging from 3 m (9.84 ft) to 60 m (197 ft), maximum predicted runup from the simulations did not exceed 2 m (6.6 ft) above MSL. Maximum flow depth from these simulations did not exceed 3.25 m (10.7 ft).

The evaluation of the maximum flood level for a PMT event also included an analysis of the 10% exceedance of the astronomical high tide and long-term sea level rise. As regulatory criteria for these components are only available for the Probable Maximum Storm Surge (PMSS), the criteria for the PMSS in Regulatory Guide 1.59 (1977) (Reference 2.4S.6-15) were adopted for the PMT analysis. Based on tide gage data for NOS Station #8772440, which is located in Freeport, Texas, the 10% exceedance of the astronomical high tide was estimated to be 3.54 ft (1.08 m) MSL (Reference 2.4S.6-16). The long-term sea level rise for this station was estimated by NOAA to be 0.171 in (4.35 mm) per year or 1.43 ft (0.44 m) per century (Reference 2.4S.6-17). The peak flood level due to a PMT event is therefore estimated to be of the order of 11.5 ft (3.52 m) MSL within the next century (i.e., 6.56 ft tsunami runup + 3.54 ft 10% exceedance of the astronomical high tide + 1.43 ft sea-level rise = 11.5 ft MSL).

A tsunami runup of 11.5 ft MSL is below the design basis flood level of 40.0 ft MSL that is postulated from a Main Cooling Reservoir (MCR) breach event (Subsection 2.4S.4). PMT is therefore not the controlling event for the design basis flood determination for STP 3 & 4 safety-related structures.

#### **2.4S.6.2 Historical Tsunami Record**

Information and data on tsunami-generating earthquakes and runup events are included in the National Geophysical Data Center (NGDC) hazards database (Reference 2.4S.6-18). The NGDC database contains information on source events and runup elevations for worldwide tsunamis from about 2000 BC to the present (Reference 2.4S.6-1). Each event in the NGDC database has a validity rating ranging from 0 to 4, with 0 for erroneous events, 1 for very doubtful events, 2 for questionable events, 3 for probable events, and 4 for definite events. Similarly, each event includes a cause code identifying the forcing mechanism (e.g., earthquake, volcano, landslide, or any combination thereof).

With respect to published literature, the publication titled “Caribbean Tsunamis: A 500-Year History from 1498-1998,” is a compendium of data and anecdotal material on tsunamis reported in the Caribbean from 1498 to 1997 (Reference 2.4S.6-19). Reference 2.4S.6-20 includes source events and runup elevations for the Caribbean Sea and Eastern United States from 1668 to 1998, respectively. The USGS has published a fact sheet showing locations of plate boundaries in the Caribbean and tsunami-generating earthquakes from 1530 to 1991 (Reference 2.4S.6-21). The map is shown in Figure 2.4S.6-2. Additionally, NOAA’s Center for Tsunami Research, in conjunction with the Pacific Marine Environmental Laboratory, publishes information and analyses on tsunami sources and tsunami events (Reference 2.4S.6-22).

Three historical tsunami runup events have been documented for the State of Texas, USA, in the NGDC database and in published literature. The first documented tsunami event for the Texas coast occurred on October 24, 1918. This tsunami was reported to be an aftershock of the  $M_w=7.5$  October 11, 1918, earthquake near Puerto Rico (Reference 2.4S.6-23, p. 73). The epicenter of the earthquake was reported at 18.5° N and 67.5° W (Reference 2.4S.6-19, p. 201), which is approximately nine miles northwest of Puerto Rico and located in the Mona Rift. As described in Reference 2.4S.6-19 (p. 201), this earthquake was “considered a terrific aftershock of the October

11 event...[with] a small wave [being] recorded at the Galveston, Texas, tide gage.” This event has a validity rating of four. The magnitude of tsunami runup was not reported.

The second documented tsunami event for the Texas coast occurred on May 2, 1922. The epicenter of the earthquake associated with this event was reported at 18.4° N and 64.9° W (Reference 2.4S.6-19, p. 201). Reference 2.4S.6-19 (p. 201) stated that “a wave with an amplitude of 64 cm was reported on a tide gage at Galveston. A train of three waves with a 45-minute period was followed in 8 hours by a 28-cm wave in a similar train of smaller waves. Parker [Reference 2.4S.6-24] associated it with an earthquake felt 4 hours earlier at Vieques, Puerto Rico.” However, according to Campbell [Reference 2.4S.6-25, p. 56], the shock had a duration of only two seconds. Therefore, the earthquake is unlikely to have been the tsunamigenic source. The validity rating of this event in the NGDC database is a two (i.e., a questionable event). No runups were documented along the Gulf coast for the primary shock of the 1922 earthquake. The surge was presumed to have been locally amplified by the inland position of the tidal gage (Reference 2.4S.6-24, p. 30). The magnitude of the 1922 earthquake or the aftershock has not been estimated.

The third documented tsunami event for the Texas coast occurred on March 27, 1964. The event was recorded on a tide gage in Freeport, Texas (Reference 2.4S.6-26). While the validity of this event was a four, estimates of the wave height vary considerably between eyewitness accounts and tide gage data. Reference 2.4S.6-26 (p. 261) notes that “in several reports from eyewitnesses in the coastal regions of Louisiana and Texas, waves up to 6 feet (2 meters) in height were observed.” However, Reference 2.4S.6-26 (p. 261) reports that the “maximum height of the recorded seiche at 0400 GMT is about seven inches (18 cm),” and that the “true wave height may have been several feet ([i.e.] about a meter).” This event coincided with the 1964 Alaska ( $M_w=9.2$ ) earthquake located between the Aleutian Trench and the Aleutian Volcanic Arc (Reference 2.4S.6-27). Additional analyses of tide gage records from the 1964 event report the maximum measured height of the low-frequency waves along the Texas coast from the Alaska earthquake ranged from 0.22 to 0.84 feet (Reference 2.4S.6-28, p. 26).

### **2.4S.6.3 Source Generator Characteristics**

Tsunamigenic source characteristics with potential to affect the US Atlantic and Gulf coasts are summarized in Reference 2.4S.6-3, several databases, and published literature as discussed in the following subsections.

#### **2.4S.6.3.1 Seismic tsunamis**

In comparison to tsunami runup events that have been documented in the Caribbean (Reference 2.4S.6-29), the Texas coast has had relatively few runup events. For example, as noted previously, Reference 2.4S.6-3 (p. ii) stated that “tsunamis generated by earthquakes do not appear to impact the Gulf of Mexico coast.” However, tsunamigenic earthquake sources that may affect the Gulf of Mexico are discussed in Reference 2.4S.6-3 (pp. 105-112). As stated in Reference 2.4S.6-3 (p. 105):

“Earthquake-generated tsunamis generally originate by the sudden vertical movement of a large area of the seafloor during an earthquake. Such movement is generated by reverse faulting, most often in subduction zones. The Gulf of Mexico basin is devoid of subduction zones or potential sources of large reverse faults. However, the Caribbean basin contains two convergence zones whose rupture may affect the Gulf of Mexico, the North Panama Deformation Belt and the Northern South America Convergent Zone.”

As stated in Reference 2.4S.6-3, source areas with potential for tsunamigenesis affecting the US Gulf Coast include the North Panama Deformation Belt and the Northern South American Convergent Zone (Table 2.4S.6-3). With respect to the North Panama Deformation Belt, Reference 2.4S.6-3 stated that:

“the largest segment of the North Panama Deformation Belt is oriented between 60°-77°. The 1882 Panama earthquake appears to have ruptured at least 3/4 of the available length of the convergence zone, and was estimated to have a magnitude of 8. While there was significant tsunami damage locally, there were no reports from the Gulf of Mexico of a tsunami from this earthquake. The low convergent rate (7-11 mm/yr) across the North Panama Deformation Belt supports long recurrence interval for large earthquakes.”

The Harvard Centroid-Moment-Tensor (CMT) catalog was searched for potential seismogenic earthquakes in the two source regions of Table 2.4S.6-3 (Reference 2.4S.6-30). The following criteria were used for searching the CMT catalog within the North Panama Deformation Belt: a date range of 01/01/1976 (i.e., the start of the database) through 11/04/2008; latitude from 9° N to 12° N; longitude from 83° W to 77° W; depth from 0 to 1000 km; and moment magnitude ( $M_w$ ) range from 6.5 to 10. The selection of a lower bound of  $M_w=6.5$  is based on criteria from Reference 2.4S.6-2 (p. 23) for a threshold moment magnitude of tsunamigenesis from earthquakes. One record was identified in the CMT catalog with these criteria. On 04/22/1991, a  $M_w=7.6$  earthquake occurred at depth of 15 km and at a latitude of 10.10° N and a longitude of 82.77° W, located about 20 mi. (32 km) offshore of the town of Limon, Costa Rica. Source parameters for the earthquake were documented as a strike of 103 degrees, a dip of 25 degrees, and a rake of 58 degrees. Source parameters for earthquakes in the North Panama Deformation Belt with moment magnitudes below 6.5 are discussed in Reference 2.4S.6-3. With respect to the far-field tsunami hazard on the South Texas coast, these additional sources are not reasonably expected to exceed the tsunamigenic potential of scenarios simulated by Reference 2.4S.6-3 and Reference 2.4S.6-4.

The following criteria were used for searching the CMT catalog within the Northern South American Convergent Zone: a date range of 1/1/1976 to 11/04/2008; latitude from 11.5° N to 14° N; longitude from 77° W to 64° W; depth from 0 to 1000 km; and moment magnitude range from 6.5 to 10. No records were identified in the CMT catalog with these criteria. By broadening the criteria to include earthquakes from  $0 < M_w < 10$ , two records were returned. The moment magnitude of the two earthquakes was 5.1. Moment magnitudes of 5.1 are below the generally accepted threshold required for seismic tsunamigenesis as defined by Reference 2.4S.6-2 (p. 23).

Therefore, the assessment of far-field tsunami hazards in this region was based on tsunami simulations in References 2.4S.6-4 and 2.4S.6-3. Reference 2.4S.6-4 performed tsunami simulations of seismic-borne tsunamis from postulated “worst-case” events using a two-dimensional depth-integrated hydrodynamic model described in Reference 2.4S.6-31. The following cases were used in the assessment (Reference 2.4S.6-4, p. 305):

1.  $M_w=9.0$  at  $66^\circ$  W and  $18^\circ$  N (Puerto Rico trench);
2.  $M_w=8.2$  at  $85^\circ$  W and  $21^\circ$  N (Caribbean Sea);
3.  $M_w=9.0$  at  $66^\circ$  W and  $12^\circ$  N; and
4.  $M_w=8.2$  at  $95^\circ$  W and  $20^\circ$  N (near Veracruz, Mexico).

The source location of Case 3 at  $66^\circ$  W and  $12^\circ$  N is cited in Reference 2.4S.6-4 (p. 305) as the North Panama Deformation Belt, but the location corresponding to  $66^\circ$  W and  $12^\circ$  N is the South Caribbean Deformed Belt (Reference 2.4S.6-3, p. 110).

Source parameters for the model cases in Reference 2.4S.6-4 were based on the formulae of Reference 2.4S.6-32. For example, source parameters for the Veracruz scenario (Reference 2.4S.6-4, p. 305) are provided in Table 2.4S.6-4. Reference 2.4S.6-4 (p. 305) stated that the model sources were aligned with local strike.

Reference 2.4S.6-4 (p. 311) concluded that “sources outside the Gulf are not expected to create a tsunami threatening to the Gulf coast.” Reference 2.4S.6-4 attributed this result primarily due to friction losses as the waves travel through the Straits of Florida and throughout islands in the Caribbean. Tsunami simulations in Reference 2.4S.6-3 complemented earlier work by Reference 2.4S.6-4, with Reference 2.4S.6-3 (p. 117) stating that:

“in general, these results are consistent with the findings of Knight (2006) [Reference 2.4S.6-4], where the far-field tsunamis generated from earthquakes located beneath the Caribbean Sea are higher along the Gulf coast than the Atlantic coast because of dissipation through the Greater Antilles islands. Conversely, tsunamis generated from earthquakes north of the Greater Antilles are higher along the Atlantic coast than the Gulf coast.”

Reference 2.4S.6-4 (p. 311) stated that one reason for this conclusion was that “the Atlantic and Gulf coasts are nearly independent since the hydrodynamic connection between basins is through the narrow Straits of Florida and through the Caribbean, where bottom friction losses appear to be large.”

Additionally, the largest deepwater wave from the Reference 2.4S.6-3 simulations was produced from the north Venezuela subduction zone. The maximum wave height from the north Venezuela subduction zone from a buoy at a depth of 250-m offshore of New Orleans, Louisiana, was estimated to be 6 cm (Reference 2.4S.6-3, p. 130, Figure 7-4e, “Station 1”).

While tsunamigenic earthquakes within the Gulf of Mexico have not been recorded, Reference 2.4S.6-4 included a tsunami simulation assuming a magnitude  $M_w=8.2$  earthquake offshore of Veracruz, Mexico. The resulting wave amplitude at the South Texas coast was about 0.35 m. Intraplate earthquakes are less common than earthquakes occurring on faults near plate boundaries, but several earthquakes in the past three decades had epicenters within the Mississippi Canyon and Fan province (Reference 2.4S.6-3). In recent time, the most severe earthquake in this region occurred on September 10, 2006. The moment magnitude was recorded as 5.8. The second largest earthquake in this region occurred on February 10, 2006 with a moment magnitude of 5.2. The United States Geological Survey (USGS) concluded that earthquakes of this magnitude are unlikely to produce any destructive tsunami (Reference 2.4S.6-33).

#### **2.4S.6.3.2 Seismic seiches**

The only documented event of a seismic seiche on the Texas coast is from the 1964 Alaska earthquake. Reference 2.4S.6-28 indicated that the horizontal acceleration associated with seismic surface waves from the Alaska shock appears to have varied markedly within North America. The amplitude of horizontal acceleration was especially large along the Gulf coast. Reference 2.4S.6-28 (p. 27) further stated that “thick deposits of sediments of low rigidity along the Gulf coast, for example, are capable of amplifying the horizontal acceleration of surface waves to a considerable extent; this accounts for the concentration of seiches that occurred along the Gulf coast.”

While the  $M_w=9.5$  magnitude 1960 earthquake in Chile might also have been expected to have caused seiches along the Texas coast, tide gages along the Gulf coast did not record any event. The  $M_w=7.8$  New Madrid earthquake that occurred on February 7, 1812 (Reference 2.4S.6-34), which is the largest earthquake recorded in the contiguous United States, produced significant seiches in the Mississippi River and in waterways along the Texas state boundary (Reference 2.4S.6-20, p. 124). However, no records exist to indicate that the 1812 New Madrid earthquake directly affected the South Texas coast or the Lower Colorado River near STP 3 & 4.

#### **2.4S.6.3.3 Volcanism-based tsunamis**

Reference 2.4S.6-3 did not cite a tsunami hazard to the Gulf coast from volcanism. For example, Reference 2.4S.6-3 stated that “far-field landslides, such as in the Canary Islands, are not expected to cause a devastating tsunami along the U.S. Atlantic coast.” Previous studies have conjectured that the eruption and collapse of the Cumbre Vieja volcano on the island of La Palma in the Canary Islands could potentially affect the coast of Florida, USA, with a 25-m wave (Reference 2.4S.6-5). A recent assessment of Reference 2.4S.6-5 was discussed in Reference 2.4S.6-3 (p. 57):

“as envisioned by Ward and Day (2001) [Reference 2.4S.6-5], a flank collapse of the volcano may drop a rock volume of up to  $500 \text{ km}^3$  into the surrounding ocean. The ensuing submarine slide, which was assumed to propagate at a speed of 100 m/s, will generate a strong tsunami with amplitudes of 25 m in Florida. In addition, [Ward and Day, 2001] claimed that the collapse of Cumbre

Vieja is imminent. In our opinion, the danger to the U.S. Atlantic coast from the possible collapse of Cumbre Vieja is exaggerated. Mader (2001) [Reference 2.4S.6-35] pointed out that Ward and Day's (2001) assumption of linear propagation of shallow water waves is incorrect, because it only describes the geometrical spreading of the wave and neglects dispersion effects. A more rigorous hydrodynamic modeling by Gisler et al. (2006) [Reference 2.4S.6-36], confirms Mader's criticism. Their simulations show significant wave dispersion and predict amplitude decay proportional to  $r^{-1}$  for a 3-dimensional model and  $r^{-1.85}$  for a 2-D model ( $r$  is distance). [Reference 2.4S.6-36] predicted [a] wave amplitude for Florida is between 1 [and] 77 cm. [Reference 2.4S.6-36 used] slightly smaller volume,  $375 \text{ km}^3$ , than Ward and Day (2001), but a much higher slide speed, that is much closer to the phase speed for tsunamis in the deep ocean (4,000 m of water)."

Further research on the La Palma event indicated that the distribution of slide blocks on the ocean bottom suggests that the collapse of Cumbre Vieja may not have been the result of a single catastrophic event, but the result of several smaller events. A recent report on potential tsunami threats to the United Kingdom concluded that "studies of the offshore turbidities [i.e., poorly sorted sediment that is deposited from a density flow of mixed water and sediment] created by landslides from the flanks of the Canary Islands suggest that these result from multiple landslides spread over periods of several days" and are therefore "likely to create tsunamis of only local concern" (Reference 2.4S.6-37, p. 23 and p. 30, respectively).

As no tsunamis have been documented in the Gulf of Mexico as a result of recent volcanic eruptions or associated mass wasting events (i.e., gravity-driven mass movement of soil, regolith, or rock moving downslope), this mechanism is not considered further as a potential source of tsunamis along the South Texas Coast.

#### **2.4S.6.3.4 Submarine slump tsunamis**

Reference 2.4S.6-3 (p. 35) cites four credible SMF source areas in the Gulf of Mexico: the Florida Escarpment, Campeche Escarpment, Northwest Gulf of Mexico, and the Mississippi Canyon (Figure 2.4S.6-3). These four SMF source areas are located in three geologic provinces: a carbonate province, a salt province, and a canyon to deep-sea fan province.

The postulated SMF sources in the carbonate province are located offshore of West Florida and in the Campeche Escarpments north of the Yucatan Peninsula (Reference 2.4S.6-3). The largest scar in this region is along the central part of the West Florida Slope and is estimated as 120 km long, 30 km wide, with a total volume of material removed of about  $1,000 \text{ km}^3$ . However, formation of the scar was believed to have occurred as a result of multiple events. Most of the sediment was estimated to have been removed before the middle of the Miocene [c. 11.6 million years ago]. Reference 2.4S.6-3 (p. 28) stated the following:

"During the Mesozoic, an extensive reef system developed around much of the margin of the Gulf of Mexico Basin by the vertical growth of reefs and carbonate shelf edge banks. This reef system is exposed along the Florida Escarpment

and the Campeche Escarpment that fringe the eastern and southern margins of this basin. These escarpments stand as much as 1,500 m above the abyssal plain floor, and have average gradients that commonly exceed 20° and locally are vertical. Reef growth ended during the Middle Cretaceous, and subsequently the platform edges have been sculpted and steepened by a variety of erosional processes.”

The salt province is located in the northwestern Gulf of Mexico. Reference 2.4S.6-3 (p. 32) stated that Geologic Long-Range Inclined Asdic (GLORIA) imagery identified 37 SMFs in the salt province and along the base of the Sigsbee Escarpment. The largest of these landslides is the East Breaks slump, which is discussed in additional detail below. With respect to the morphology of the salt province, Reference 2.4S.6-3 (pp. 27-28) stated the following:

“Salt deposited in the late Jurassic Gulf of Mexico basin, the Louann salt, originally underlay large parts of Louisiana, southern Texas, and the area offshore of Mexico in the Bay of Campeche. As sediment eroded from the North American continent was deposited on this salt sheet throughout the Mesozoic and Cenozoic, the increased load caused the salt to flow with it migrating southward from the source area into the northern Gulf of Mexico. Presently the Louann salt underlies large parts of the northern Gulf of Mexico continental shelf and continental slope. South of Louisiana and Texas, the Sigsbee Escarpment is a pronounced cliff that marks the seaward limit of the shallowest salt tongue. As the salt is loaded, it flows both seaward and also upward through the overlying sediment column as cylindrical salt domes. The morphology of the salt sheet varies considerably across the margin. Salt domes are most common under the continental shelf, and most of the original salt sheet between individual domes in this region has been removed in response to the sediment loading, and migrated farther seaward.”

Other SMFs identified in the salt province have areas that are an order of magnitude lower than the East Breaks slump (Reference 2.4S.6-3), and are not further considered.

Three canyon to deep-sea fan systems were formed during the Pliocene and Pleistocene: the Mississippi, Eastern Mississippi, and Bryant systems (Figure 2.4S.6-3). The Mississippi system is the largest of the three systems, though Reference 2.4S.6-3 states that the resumption of hemipelagic sedimentation at the head of the Mississippi Canyon by 7500 yr BP indicates that the largest of the landslide complexes ceased being active by the middle of the Holocene. The largest SMF in the complex covers approximately 23,000 km<sup>2</sup> and reaches 100 m in thickness, with a volume estimated to be about 1,750 km<sup>3</sup>. GLORIA sidescan sonar data suggests that this feature consists of at least two separate events (Reference 2.4S.6-3).

The Eastern Mississippi and Bryant Canyon systems are smaller than the Mississippi Canyon system. The Eastern Mississippi system has a deposit that is “approximately 154 km long, as much as 22 km wide, and covers an area of 2,410 km<sup>2</sup>” (Reference

2.4S.6-3, p. 34). With respect to the Bryant system, Reference 2.4S.6-3 (pp. 33-34) states that

“The Bryant Canyon system was immediately downslope of a shelf edge delta system, and failure of this system has been proposed as the explanation for thick chaotic deposits in mini basins along the path of this canyon system. Debris from the failure of the shelf edge delta was transported down the Bryant Canyon system, but these landslide deposits predate and are buried by the smaller landslides off the mini-basin walls.”

#### **2.4S.6.4 Tsunami Analysis**

Tsunami modeling was conducted for a tsunami originating at the location of the East Breaks slump near the South Texas coast. For all scenarios, the tsunamigenic source was a SMF. As with Reference 2.4S.6-12 and Reference 2.4S.6-13, a series of scaled dipolar initial conditions were used for bracketing a conservative range of initial wave heights. Hydrodynamic simulations were modeled using a series of codes known as the Method of Splitting Tsunami (MOST) (References 2.4S.6-8). For all model simulations, maximum runup along the South Texas coast did not exceed 2 m (6.56 ft) above Mean Sea Level (MSL).

The following paragraphs discuss the geologic setting of the East Break slump, followed by discussion of hydrodynamic simulations with MOST.

The East Breaks slump is located approximately 88.2 mi (142 km) to the southeast of STP 3 & 4 (Figure 2.4S.6-4). The coordinates of the slump are approximately 27.57° N and 95.64° W. The slump is comprised of an eastern lobe and a western lobe. Reference 2.4S.6-38 (p. 2) stated that “the western and eastern lobes are thought to have formed by two different processes, and actually at two different, but relatively close, time periods. The western lobe formed as slump and debris deposits traveled downslope. The eastern lobe is more consistent with turbidity flow currents in the upper parts of the slide and leveed channels in the middle and lower portions of the slide.” Further, Reference 2.4S.6-38 (p. 3) stated that “the eastern lobe appears more channelized and consists of density flow-type fill with few large slump and intact blocks. The western lobe, therefore, carried the bulk of the failed material and the energy level of the failure was much greater.” As the eastern lobe was unlikely to have influenced tsunamigenesis, only the western lobe was used for the simulations.

The age of the East Breaks slump is not precisely known. Reference 2.4S.6-39 (p. 366) stated that the most recent mass wasting event responsible for the formation of the western lobe occurred about 16,000 yr BP, and after the formation of the bulk of the eastern lobe. Reference 2.4S.6-7 stated that “the East Breaks Slide is a site of [sea level] lowstand instability, and seismic [reflection] data shows repeated slope failure in this area. During late Quaternary lowstands of sea level, large deltas built up along the Texas-Louisiana shelf margin, and the present continental shelf [became] exposed as a subaerial coastal plain.” Reference 2.4S.6-7 also stated that “it is clear that most sliding on the Texas-Louisiana slope occurred during the late Pleistocene [c. 10,000 - 29,000 years BP] lowstands of sea level when sedimentation rates on the upper slope were high.”

With respect to stability, Reference 2.4S.6-3 notes that information on the age of landslides in the salt province is limited. Most landslides appear to have been active during oxygen isotope stages 2, 3, and 4 (18,170-71,000 yr BP) when salt movement due to sediment loading was most active. The age of the most recent landslide is less well established. For example, Reference 2.4S.6-7 stated that that no major SMFs have occurred in the northwestern Gulf of Mexico in the Holocene (i.e., the last 10,000 years). Reference 2.4S.6-7 (p. 309) stated:

"Studies of submarine slides invariably prompt the question: Is the slope now completely stabilized? It is clear that most sliding on the Texas-Louisiana slope occurred during the late Pleistocene lowstands of sea level when sedimentation rates on the upper slope were high. No major Holocene slides have been documented. Low rates of deposition may be a primary reason for the present stability over much of the upper slope, and a further indication that sediments are relatively stable."

However, Reference 2.4S.6-3 suggests the occurrence of at least one landslide during the Holocene, with "one unpublished age date of a sample below a thin landslide deposit (<3 m thick) indicates that it is younger than 6,360 yr BP." Therefore, no major SMFs have been documented for the salt province in over 6,300 years.

With respect to dimensions of the East Breaks slump scar, estimates of width, length, area, and volume have varied with different studies. For example, Reference 2.4S.6-40 stated that the slump "consists of a 20-km wide head scarp initiated along the 150-meter isobath, a 55 km long erosional chute, ending in a 95x30 km accretionary lobe. Total extent of the feature is 160 km from the shelf edge to a depth of 1,500 m" and "slumped deposits extend over a 3,200-km<sup>2</sup> area with a volume on the order of 50-60 km<sup>3</sup>." Reference 2.4S.6-7 stated that "the East Breaks Slide is a prominent mass-transport feature. Revised bathymetry shows that the slide originated on the upper slope (200-1000 m), in front of a sandy late Wisconsinan shelf-margin delta, where the gradient is up to 3°. It was deposited in a middle slope position (1000-1500 m) where the gradient is about 0.5°. Side-scan sonar data indicates that the slide is a strongly backscattering feature extending more than 110 km downslope from the shelf edge." Reference 2.4S.6-3 (p. 32) stated that "the largest of these failures occurs in the northwestern Gulf of Mexico, is 114 km long, 53 km wide, covers about 2,250 km<sup>2</sup>, and has been interpreted to consist of at least two debris flows."

Source parameters for the East Breaks slump were estimated using three arc-second bathymetry data from the National Geophysical Data Center (NGDC) (Reference 2.4S.6-41). Source parameters, including slump width, length, and thickness, were estimated using a Geographic Information Systems (GIS) environment (Figure 2.4S.6-5). Slump width was estimated to be approximately 13.4 km. The length of the erosional chute was estimated to about 42 km. Based on a transect across the erosional chute, slump thickness was estimated to be about 100 m (i.e., see Path Profile A to A' in Figure 2.4S.6-5). With respect to slope, Reference 2.4S.6-40 stated that "initial failure of the slump took place on very low angle slopes of less than two degrees while present slump deposits have an average seafloor slope of one-degree." While a vertical drop of 850 m over a length of 42 km indicates a bed slope of

approximately 1.1 degrees, local bed slopes measured in GIS using a longitudinal transect along the erosional chute indicate a local maximum slope of about 1.95°. Therefore, a maximum local slope of 2° was used for a conservative estimate. Similarly, initial depth of the slide was estimated conservatively using the 200-m and 1000-m bathymetry contour elevations. Therefore, initial depth was estimated to be 600 m (i.e., (200 m + 1000 m)/2) (Figure 2.4S.6-5). Total length of the slide was taken from Reference 2.4S.6-3 as 114 km.

With respect to simulations, tsunami modeling was performed with MOST. Validation of the MOST code is well established (Reference 2.4S.6-9). MOST is based on the following three phases of long wave evolution (Reference 2.4S.6-8):

- (i) A “Deformation Phase” that generates the initial conditions for a tsunami by simulating ocean floor and corresponding free surface changes due to a forcing mechanism;
- (ii) A “Propagation Phase” that propagates the generated tsunami across the deep ocean using Nonlinear Shallow Water (NSW) wave equations; and
- (iii) An “Inundation Phase” that simulates the shallow ocean behavior of a tsunami by extending the NSW calculations using a multi-grid runup algorithm to predict coastal flooding and inundation.

Specification of an initial deformation condition was based on scaling a dipole wave (i.e., a wave with a dipolar structure). A dipole wave is similar to the structure of an N-wave (i.e., a tsunami with a leading negative or depression wave followed by a positive elevation wave). An initial dipole wave is characteristic of tsunamis from submarine landslides, and possibly all tsunamis (Reference 2.4S.6-14).

After specifying an initial deformation condition, the propagation phase is based on a simplified form of the Navier-Stokes equations referred to as the nonlinear shallow water (NSW) equations (Reference 2.4S.6-8). The NSW equations are solved numerically with a finite difference algorithm and a series of nested grids (Reference 2.4S.6-42).

Since tsunami wavelength becomes shorter during shoaling, a series of nested grids are required for maintaining resolution of the wave with decreasing water depth. Therefore, three grids (i.e., A, B and C) were used for the MOST simulations (Figure 2.4S.6-6). The grids were derived from NGDC topography and bathymetry data (Reference 2.4S.6-41). Grid spacing between nodes was equal to 12 arc-seconds, 6 arc-seconds, and 6 arc-seconds, respectively.

MOST uses a moving boundary calculation for estimating tsunami runup onto dry land. Details of the moving boundary are discussed in Reference 2.4S.6-43. While friction factors are not used in the propagation phase of MOST, a friction factor must be specified for the inundation phase. Following sensitivity simulations, this value was set equal to 0.01 (i.e.,  $n=0.1$ ). Reference 2.4S.6-2 states that “several studies show that an unsteady flow during runup is not very sensitive to changes in the roughness coefficient”, and that “any moving boundary computation induces numerical friction

near the tip of the climbing wave (except in a Lagrangian formulation).” However, this value was selected based on a series of sensitivity tests, where the most conservative value that could be used without numerical instability over the full duration of the simulation was selected.

Initial wave heights (i.e., initial elevation of the depression wave due to a slump) were estimated using the slump center of mass motion model described in Reference 2.4S.6-10 and Reference 2.4S.6-11. Source parameters documented in the paragraphs above and in Figure 2.4S.6-5 were used for estimating initial wave height. Specific gravity of the slump mass was assumed to be equal to 2. The 100-m thickness (T) with respect to the 600-m initial depth (h) ( $T/h=0.17$ ) and the thickness relative to the 42 km length (b) of the erosional chute ( $T/b=0.002$ ) suggests initial wave height from the East Breaks slump would be relatively small. Using the NGDC bathymetry data (Figure 2.4S.6-5), initial wave height for the East Breaks slump was estimated to be 7.9 m. Considering variability in interpreting landslide dimensions, the estimate of 7.9 m is similar to the “tsunami wave on the order of 7.6 meters” predicted by Reference 2.4S.6-40.

As noted in the preceding paragraphs, estimates of slump dimensions can vary considerably with different interpretations. Therefore, estimates of initial conditions (i.e., wave height and shape) are not easily replicable between investigators. Consequently, after establishing a range of possible wave heights from scaling studies in Reference 2.4S.6-11 and Reference 2.4S.6-14, initial dipole conditions were developed for the East Breaks slump simulations by using SMF wave shapes developed for other SMF events. These events include the Palos Verdes (PV) landslide in Southern California (Reference 2.4S.6-12) and the 1998 Papua New Guinea (PNG) slump in the Sandaun Province (Reference 2.4S.6-13).

Scaled initial conditions were used for the simulations as relatively little data exists for SMFs, and the PV and PNG events have been tested extensively by the tsunami community (Reference 2.4S.6-13 and Reference 2.4S.6-14). Four scenarios were modeled as candidate PMT events. Candidate PMT events included waves with high initial wave heights relative to wavelength (i.e., steep waves), and waves with high initial wave heights relative to width. Minimum (negative) and maximum (positive) elevations of the initial wave deformations are listed in Table 2.4S.6-5. Steep wave scenarios included PV and PV(x20); wide wave scenarios included PNG and a hypothetical “Monster” condition. PV, which has a deformation area of  $411 \text{ km}^2$ , was developed as a minimum estimate of initial wave height for the East Breaks slump (Table 2.4S.6-5). PV(x20), which is PV scaled in elevation by twenty times and with a slightly smaller deformation area of  $387 \text{ km}^2$ , was developed as a maximum estimate of initial wave height for the East Breaks slump. PNG is scaled directly from the Papua New Guinea submarine slump described in Reference 2.4S.6-13, and has a deformation area of  $879 \text{ km}^2$ , which is about twice as large as PV. A hypothetical “Monster” condition was also developed as a complementary case for the East Breaks slump. The hypothetical “Monster” condition has not been tested by the tsunami community. Rather, the hypothetical “Monster” case was developed as a complementary case for the East Breaks slump to test a very wide initial wave (i.e.,

initial deformation area of 9932 km<sup>2</sup> or 3835 mi<sup>2</sup>). All initial conditions were located at the centroid of the slump and oriented to relative to the slump direction.

MOST output includes maximum runup estimates (i.e., maximum inland elevation inundated by the tsunami above MSL). Maximum runup ranges from 1 to 2 m (3.28 to 6.56 ft, respectively) MSL for the South Texas Coast near STP 3 & 4 (Table 2.4S.6-5). The simulations indicate that a landslide tsunami originating from the East Breaks slump location would be unlikely to cross the barrier islands and produce a runup in excess of 2 m (6.56 ft) MSL. Plots of maximum wave amplitude relative to South Texas coast bathymetry are shown for PV, PV(x20), PNG, and the hypothetical "Monster" cases in Figure 2.4S.6-15, Figure 2.4S.6-17, Figure 2.4S.6-19, and Figure 2.4S.6-21, respectively. Time series of wave amplitude for a buoy located near the South Texas Coast for the PV, PV(x20), PNG, and hypothetical "Monster" are shown in Figure 2.4S.6-16, Figure 2.4S.6-18, Figure 2.4S.6-20, and Figure 2.4S.6-22, respectively.

Maximum drawdown was estimated at a buoy located at depth of 8.1 m and approximately 1 mi offshore of the South Texas coast (Figure 2.4S.6-4). At this location, significant drawdown of the water surface below MSL occurred for initial negative waves for the PV(x20) and hypothetical "Monster" scenarios. Maximum drawdown for the PV(x20) case had a duration of about 21 minutes, with a peak negative wave elevation of about -1.5 m (-4.9 ft) (Figure 2.4S.6-18). Maximum drawdown (i.e., below MSL) for the hypothetical "Monster" case had a duration of about 23 minutes, with a peak negative wave elevation of about -2.5 m (-8.2 ft) (Figure 2.4S.6-22). Therefore, maximum drawdown levels are not expected to impact any safety-related facilities at STP 3 & 4.

#### **2.4S.6.5 Tsunami Water Levels**

Reference 2.4S.6-3 (p. 34) stated that subaerial landslides, volcanogenic sources, and nearfield intraplate earthquakes are unlikely to be the causative tsunami generator for damaging tsunamis in the Gulf of Mexico region. Reference 2.4S.6-3 also stated that far-field "tsunamis generated by earthquakes do not appear to impact the Gulf of Mexico coast." Simulations by Reference 2.4S.6-4 of postulated "worst-case" seismic events reported a tsunami near STP 3 & 4 with a shoreline amplitude of 0.15 m.

As far-field tsunamis are unlikely to impact the South Texas coast, the PMT for STP Subsection 2.4S.6 is defined as a tsunami occurring from a near-field submarine landslide near the East Breaks slump. Using the MOST code (Reference 2.4S.6-8), a series of scaled initial conditions were used to assess the near-field hazard of tsunami generation from submarine landslides to the STP 3 & 4 site. For scenarios with wave heights ranging from - 140 m (-459 ft) to 60 m (197 ft) and deformation areas ranging from 410 km<sup>2</sup> to 9932 km<sup>2</sup>, tsunami waves from the SMFs were diffused rapidly by the continental shelf offshore of the South Texas coast. The remaining wave energy that reached the South Texas coast was largely reflected by the barrier islands. For example, maximum predicted runup from the simulations did not exceed 2 m. Maximum flow depth from the simulations, which occurred at the shoreline, did not exceed 3.25 m. Maximum rundown did not exceed 2.5 m about 1 mi offshore of the South Texas coast.

The initial deformation conditions listed in Table 2.4S.6-5 plausibly exceed wave heights from propagating tsunamis that may occur due to landslides in remote areas of the Gulf of Mexico. For example, relative to the location of STP 3 & 4, most SMF sources in the Gulf of Mexico are mid-field to far-field sources (i.e., source locations over 200 km away) (Figure 2.4S.6-3). The distance from STP 3 & 4 to the East Breaks slump is 142 km (88.2 mi). The distance from STP 3 & 4 to Bryant Canyon is 517 km (321.2 mi). The distance from STP 3 & 4 to Mississippi Canyon and the Eastern Mississippi Canyon/Fan is 640 km (397.7 mi) and 709 km (440.6 mi), respectively. The distance from STP 3 & 4 to the Campeche Escarpment and Bay of Campeche is 873 km (542.5 mi) and 953 km (592.2 mi), respectively. The distance from STP 3 & 4 to the Florida escarpment is 1169 km (726.4 mi). Since landslide waves tend to be steep (i.e., high initial wave height relative to wavelength) and are prone to breaking, wave heights at the East Breaks slump from mid-field and far-field sources are not expected to exceed the simulated initial conditions. As shown with the simulations, diffusion and energy dissipation from large SMF events is likely to be significant. Therefore, potential runup from these events is likely to be lower than the scenarios modeled for the East Breaks slump, and additional landslide scenarios in the Gulf of Mexico are not further considered.

As discussed earlier, the maximum flood level for a PMT event also included an analysis of the 10% exceedance of the astronomical high tide and long-term sea level rise. As regulatory criteria for these components are only available for the Probable Maximum Storm Surge (PMSS), the criteria for the PMSS in Regulatory Guide 1.59 (1977) (Reference 2.4S.6-15) were adopted for the PMT analysis. Based on tide gage data for NOS Station #8772440, the 10% exceedance of the astronomical high tide was estimated to be 3.54 ft MSL (Reference 2.4S.6-16). The long-term sea level rise for this station was estimated by NOAA to be 1.43 ft per century (Reference 2.4S.6-17). The peak flood level due to a probable maximum tsunami event is therefore estimated to be of the order of 11.5 ft MSL within the next century.

With respect to the assumption of the MSL datum (or NGVD 29) shift relative to actual mean sea level from tidal measurements, it should be noted that the Freeport, Texas, tide gage does not have a published or official NGVD29 orthometric height mark. Since the one mark that does exist suggests the difference between MSL (or NGVD 29) to actual mean sea level is small (i.e., within  $\pm 0.2$  ft of the Mean Lower-Low Water datum), the shift to MSL (or NGVD 29) should be considered as a reasonable approximation of the actual value.

Based on the discussion above, it is concluded that the probable maximum tsunami event will not be the controlling design basis flood event for STP 3 & 4 because the postulated flood level is lower than the design basis flood elevation of 40.0 feet MSL predicted for a hypothetical breach event of the MCR embankment as described in Section 2.4S.4. Coincident wind waves are not considered in the analysis since it is evident that the PMT event will have no flooding impacts on safety-related facilities of STP 3 & 4.

#### 2.4S.6.6 Hydrography and Harbor or Breakwater Influences on Tsunami

Because the STP 3 & 4 site is over fifteen miles inland from the South Texas coast and barrier islands, and the postulated maximum flood level of no more than 11.5 ft MSL due to the PMT event is lower than the site grade elevations of 32 ft MSL to 36.6 ft MSL for the power block area of STP 3 & 4, there will be no local onsite effects associated with different tsunami types, including breaking waves, bores, or any resonance effects that would result in higher tsunami runup on the safety-related facilities. Therefore, no additional analysis of the translation of tsunami waves from offshore generator locations to the site is warranted.

#### 2.4S.6.7 Effects on Safety-Related Facilities

The postulated maximum flood level of no more than 11.5 ft MSL due to the PMT event is lower than the site grade elevations of 32 ft MSL to 36.6 ft MSL for the power block area of STP 3 & 4. Therefore, the PMT event will have no flooding impacts on safety-related facilities or the design basis functions of STP 3 & 4, and there will be no impact of debris and water-borne projectiles and impacts of sediment erosion and deposition on the safety-related facilities of STP 3 & 4.

#### 2.4S.6.8 References

- 2.4S.6-1 "Tsunami Hazard Assessment at Nuclear Power Plant Sites in the United States of America." Prasad, R. and Pacific Northwest National Laboratory (PNNL), NUREG CR-6966, PNNL-17397, Nuclear Regulatory Commission, Draft Report for Comment, Revision: August 2008.
- 2.4S.6-2 "Scientific and Technical Issues in Tsunami Hazard Assessment of Nuclear Power Plant Sites," González et al., F.I., Bernard, E., Dunbar, P., Geist, E., Jaffe, B., Kanoglu, U., Locat, J., Mofjeld, H., Moore, A., Synolakis, C.E., Titov, V. and R. Weiss (Science Review Working Group), National Oceanic and Atmospheric Administration (NOAA) Technical Memorandum OAR Pacific Marine Environmental Laboratory 136, 2007.
- 2.4S.6-3 "Evaluation of Tsunami Sources with the Potential to Impact the U.S. Atlantic and Gulf Coasts - A Report to the Nuclear Regulatory Commission: U.S. Geological Survey Administrative Report," Atlantic and Gulf of Mexico Tsunami Hazard Assessment Group, Revision: August 22, 2008.
- 2.4S.6-4 "Model Predictions of Gulf and Southern Atlantic Coast Tsunami Impacts from a Distribution of Sources," Knight, B. 2006, Science of Tsunami Hazards 24(2): 304-312.
- 2.4S.6-5 "Cumbre Vieja Volcano - Potential Collapse and Tsunami at La Palma, Canary Islands," Ward, S. N. and S. Day. 2001. Geophysical Research Letters 28(17): 3397-3400.

- 2.4S.6-6 "Geomorphology and age of the Oxygen isotope stage 2 (last lowstand) sequence boundary on the northwestern Gulf of Mexico continental shelf," Simms, A.R., Anderson, J.B., Milliken, K.T., Taha, Z.P., Wellner, in Seismic Geomorphology: Applications to Hydrocarbon Exploration and Production, Davies, R.J., Posamentier, H.W., Wood, L. J. & Cartwright, J. A. (eds.), Geological Society, London, Special Publications, 277: 29-46, 2007.
- 2.4S.6-7 "Sedimentary Features of the South Texas Continental Slope as Revealed by Side-Scan Sonar and High-Resolution Seismic Data," Rothwell, R.G., Kenyon, N.H. and B.A. McGregor, The American Association of Petroleum Geologists Bulletin 75(2): 298-312, 1991.
- 2.4S.6-8 "Implementation and testing of the Method of Splitting Tsunami (MOST) model," Titov, V.V., and F.I. González et al., NOAA Technical Memorandum ERL PMEL112, Pacific Marine Environmental Laboratory, 1997.
- 2.4S.6-9 "Tsunami Science Before and Beyond Boxing Day 2004," Synolakis, C.E. and E.N. Bernard, Philosophical Transactions of the Royal Society 64: 2231-2265, 2006.
- 2.4S.6-10 "Tsunami Features of Solid Block Underwater Landslides," Watts, P., Journal of Waterway, Port, Coastal, and Ocean Engineering 126(3): 144-152, 2000.
- 2.4S.6-11 "Tsunami Generation by Submarine Mass Failure, Part II, Predictive Equations and Case Studies," Watts, P., Grilli, S.T., Tappin, D.R. and G.J. Fryer, Journal of Waterway, Port, Coastal, and Ocean Engineering 131(6): 298-310, 2005.
- 2.4S.6-12 "Tsunami Hazards in Southern California," Borrero, J.C., Ph.D. Thesis, University of Southern California, 2002.
- 2.4S.6-13 "The Slump Origin of the 1998 Papua New Guinea Tsunami," Synolakis, C.E., Bardet, J.-P., Borrero, J.C., Davies, H.L., Okal, E.A., Silver, E.A., Sweet, S., and D.R. Tappin, Proceedings: Mathematical, Physical and Engineering Sciences 458(2020): 763-789, 2002.
- 2.4S.6-14 "Tsunami and Seiche," Synolakis, C. E. 2004 from Earthquake Engineering Handbook, edited by Chen, W. F. and C. Scawthorn, CRC Press. 9-1 to 9-90.
- 2.4S.6-15 "Design Basis Floods for Nuclear Power Plants," U.S. Nuclear Regulatory Commission, Regulatory Guide 1.59, Revision 2, 1977.
- 2.4S.6-16 "NOS Station #8772440, Freeport - Verified Historic Tide Data," National Oceanic and Atmospheric Administration (NOAA), available at [http://tidesandcurrents.noaa.gov/data\\_menu.shtml?stn=8772440%20Freeport,%20TX&type=Historic+Tide+Data](http://tidesandcurrents.noaa.gov/data_menu.shtml?stn=8772440%20Freeport,%20TX&type=Historic+Tide+Data), accessed August 19, 2008.

- 2.4S.6-17 "NOS Station #8772440, Freeport - Sea Level Trends." National Oceanic and Atmospheric Administration (NOAA), 2008, available at [http://tidesandcurrents.noaa.gov/sltrends/sltrends\\_station.shtml?stnid=8772440%20Freeport.%20TX](http://tidesandcurrents.noaa.gov/sltrends/sltrends_station.shtml?stnid=8772440%20Freeport.%20TX), accessed August 19, 2008.
- 2.4S.6-18 "Tsunami Data at NGDC," National Geophysical Data Center/World Data Center. Available at <http://www.ngdc.noaa.gov/hazard/tsu.shtml>, accessed November 22, 2008.
- 2.4S.6-19 "Caribbean Tsunamis: A 500-Year History from 1498-1999. Kluwer Academic Publishers," O' Loughlin, K. F. and J. F. Lander. 2003. The Netherlands. 280 pp.
- 2.4S.6-20 "Tsunamis and Tsunami-Like Waves of the Eastern United States," Science of Tsunami Hazards 20(3): 120-157, Lockridge, P. A., Lowell, S. W., and J. F. Lander. 2002.
- 2.4S.6-21 "Improving Earthquake and Tsunami Warnings for the Caribbean Sea, the Gulf of Mexico, and the Atlantic Coast," USGS Fact Sheet 2006-3012, United States Geological Survey, 2006.
- 2.4S.6-22 "NOAA Center for Tsunami Research," Pacific Marine Environmental Laboratory (PMEL). Available at <http://nctr.pmel.noaa.gov/>, accessed November 23, 2008.
- 2.4S.6-23 "A Brief History of Tsunamis in the Caribbean Sea. Science of Tsunami Hazards," 20(2): 57-94, Lander, J. F., Whiteside, L. S., and P. A. Lockridge, 2002.
- 2.4S.6-24 "Unusual Tide Registration of Earthquake," Parker, W.E. 1922. Bulletin of the Seismological Society in America, pp. 28-30.
- 2.4S.6-25 "Earthquake History of Puerto Rico. Seismicity Investigation." Appendix I, Part A, An Earthquake History of Puerto Rico, Aguirre Nuclear Power Plant, Weston Geophysical Research," Campbell, J.B., 1972, Weston, Massachusetts.
- 2.4S.6-26 "Alaska Earthquake of 27 March 1964: Remote Seiche Stimulation. Science 145: 261-262," Donn, W. L. 1964.
- 2.4S.6-27 "Historical Earthquakes, Prince William Sound, Alaska." United States Geological Survey, Available at [http://earthquake.usgs.gov/regional/states/events/1964\\_03\\_28.php](http://earthquake.usgs.gov/regional/states/events/1964_03_28.php), accessed April 27, 2007.
- 2.4S.6-28 "Seismic Seiches in Bays, Channels, and Estuaries, from The Great Alaska Earthquake of 1964: Oceanography and Coastal Engineering," McGarr, A. and R. C. Vorhis. 1972. National Academy of Sciences, Washington, D.C. 25-28.

- 2.4S.6-29 "Assessment of Source Probabilities for Potential Tsunamis Affecting the U.S. Atlantic Coast," Parsons, T., Geist, E.L., in press, Marine Geology, doi:10.1016/j.margeo.2008.08.005.
- 2.4S.6-30 "Global Centroid Moment Tensor (CMT)." Available at <http://www.globalcmt.org/>, accessed November 21, 2008.
- 2.4S.6-31 "Numerical Modeling of the Global Tsunami: Indonesian Tsunami of 26 December 2004", Kowalik, Z., Knight, W., Logan, T. and P. Whitmore, Science of Tsunami Hazards 23(1): 40-56, 2005.
- 2.4S.6-32 "Surface Deformation Due to Shear and Tensile Faults in a Half-Space." Okada, Y., Bulletin of the Seismological Society of America 75(4): 1135-1154, 1985.
- 2.4S.6-33 "Magnitude 5.8 Gulf of Mexico Earthquake of 10 September 2006." National Earthquake Information Center, United States Geological Survey, Available at <http://earthquake.usgs.gov/eqcenter/eqinthenews/2006/usslav/#summary>, accessed December 02, 2008.
- 2.4S.6-34 "Magnitudes and locations of the 1811-1812 New Madrid, Missouri, and the 1886 Charleston, South Carolina, Earthquakes," Bakun, W. H. and M. G. Hopper, 2004, Bulletin of the Seismological Society of America 94(1): 64-75.
- 2.4S.6-35 "Modeling the La Palma Landslide Tsunami," Mader, C.L., Science of Tsunami Hazards 19(3): 150-170, 2001.
- 2.4S.6-36 "SAGE calculations of the tsunami threat from La Palma," Gisler, G., Weaver, R. and M.L. Gittings, 2006, Science of Tsunami Hazards 24(4): 288-301.
- 2.4S.6-37 "The Threat Posed by the Tsunami to the UK," British Geology Society, 2005. Study commissioned by Debra Flood Management, 133 pp.
- 2.4S.6-38 "Addressing the Challenges in the Placement of Seafloor Infrastructure on the East Breaks Slide-A Case Study: The Falcon Field (EB 579/623)," Hoffman, J.S., Kaluza, M.J., Griffiths, R., Hall, J. and T. Nguyen, Northwestern Gulf of Mexico, Offshore Technology Conference 16748, 2004.
- 2.4S.6-39 "Downslope Sediment Transport Processes and Sediment Distributions at the East Breaks, northwest Gulf of Mexico." Piper, J.N., and Behrens, in Proceedings of the 23rd Annual Gulf Coast Section SEPM Research Conference, Houston, Texas, pp. 359-385, 2003.
- 2.4S.6-40 "East Breaks Slump, Northwest Gulf of Mexico." Offshore Technology Conference, OTC paper 12960, Trabant, P., Watts, P., Lettieri, F. and G. Jamieson, 2001.

- 2.4S.6-41 National Geophysical Data Center (NGDC), 2008. "Bathymetry, Topography, and Relief," National Oceanic and Atmospheric Administration (NOAA), available at <http://www.ngdc.noaa.gov/mgg/bathymetry/relief.html>, accessed October 5, 2008.
- 2.4S.6-42 Titov, V.V. and C.E. Synolakis, 1998. "Numerical Modeling of Tidal Wave Runup." Journal of Waterway, Port, Coastal, and Ocean Engineering 124(4): 157- 171.
- 2.4S.6-43 Titov, V.V., 1997, Numerical Modeling of Long Wave Runup, Ph.D. Thesis, University of Southern California, Los Angeles, California, 141 pp.

**Table 2.4S.6-1 Approximate range of tsunami parameters in the deep ocean (Reference 2.4S.6-2).**

<u>Parameter</u>	<u>Minimum</u>	<u>Maximum</u>
<u>Depth</u>	<u>1000 m</u>	<u>5000 m</u>
<u>Period</u>	<u>5 min</u>	<u>60 min</u>
<u>Amplitude</u>	<u>0.01 m</u>	<u>1 m</u>
<u>Wavelength</u>	<u>30 km</u>	<u>800 km</u>
<u>Speed</u>	<u>0.10 km/s</u>	<u>0.22 km/s</u>
<u>Max Current</u>	<u>0.05 cm/s</u>	<u>9.9 cm/s</u>

**Table 2.4S.6-2 Approximate range of tsunami parameters in shallow water (Reference 2.4S.6-2).**

<u>Parameter</u>	<u>Minimum</u>	<u>Maximum</u>
<u>Depth</u>	<u>10 m</u>	<u>1000 m</u>
<u>Period</u>	<u>5 min</u>	<u>60 min</u>
<u>Amplitude</u>	<u>1 m</u>	<u>10 m</u>
<u>Wavelength</u>	<u>3 km</u>	<u>356 km</u>
<u>Speed</u>	<u>0.01 km/s</u>	<u>0.10 km/s</u>
<u>Max Current</u>	<u>9.9 cm/s</u>	<u>990 cm/s</u>

**Table 2.4S.6-3 Areas of potential seismic tsunamigenesis in the Caribbean (Reference 2.4S.6-3, pp. 105 and 107).**

<u>Caribbean Source</u>	<u>Latitude (° N)</u>	<u>Longitude (° W)</u>
<u>North Panama Deformation Belt</u>	<u>9-12</u>	<u>83-77</u>
<u>Northern South American Convergent Zone</u>	<u>11.5-14</u>	<u>77-64</u>

**Table 2.4S.6-4 Source parameters for Veracruz scenario.**

<u>Epicenter</u>	<u>M<sub>w</sub></u>	<u>Rupture Length (km)</u>	<u>Width (km)</u>	<u>Depth (km)</u>	<u>Strike (°)</u>	<u>Dip (°)</u>	<u>Rake (°)</u>	<u>Max slip (m)</u>
<u>20° N, 265° E</u>	<u>8.2</u>	<u>200</u>	<u>70</u>	<u>5</u>	<u>135</u>	<u>20</u>	<u>90</u>	<u>2</u>

Table 2.4S.6-5 Initial wave deformation characteristics and maximum runup for simulations.

<u>Case</u>	<u>Deformation Area (sq. km)</u>	<u>Dipole Initial Minimum (m below MSL)</u>	<u>Dipole Initial Maximum (m below MSL)</u>	<u>Maximum Runup (m above MSL)</u>	<u>Figure Reference</u>
<u>PV</u>	<u>411</u>	<u>-7</u>	<u>3</u>	<u>1</u>	<u>2.4S.6-7;</u> <u>2.4S.6-8</u>
<u>PV(x20)</u>	<u>387</u>	<u>-140</u>	<u>60</u>	<u>2</u>	<u>2.4S.6-9;</u> <u>2.4S.6-10</u>
<u>PNG</u>	<u>879</u>	<u>-20</u>	<u>16</u>	<u>2</u>	<u>2.4S.6-11;</u> <u>2.4S.6-12</u>
<u>Monster</u>	<u>9932</u>	<u>-38</u>	<u>27</u>	<u>2</u>	<u>2.4S.6-13;</u> <u>2.4S.6-14</u>



Figure 2.4S.6-1 Location Map of STP 3 & 4 from the Gulf Coast and Colorado River.

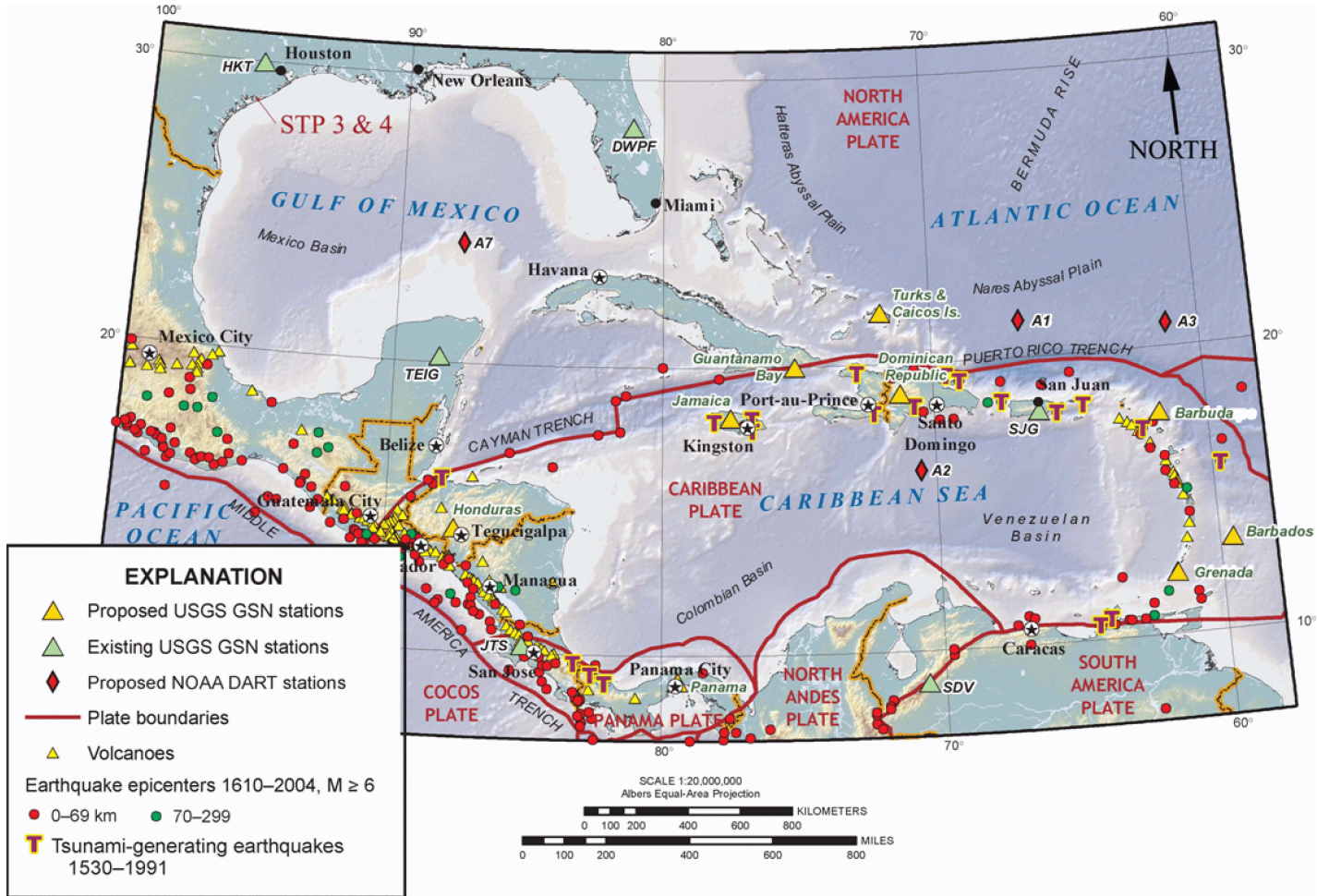
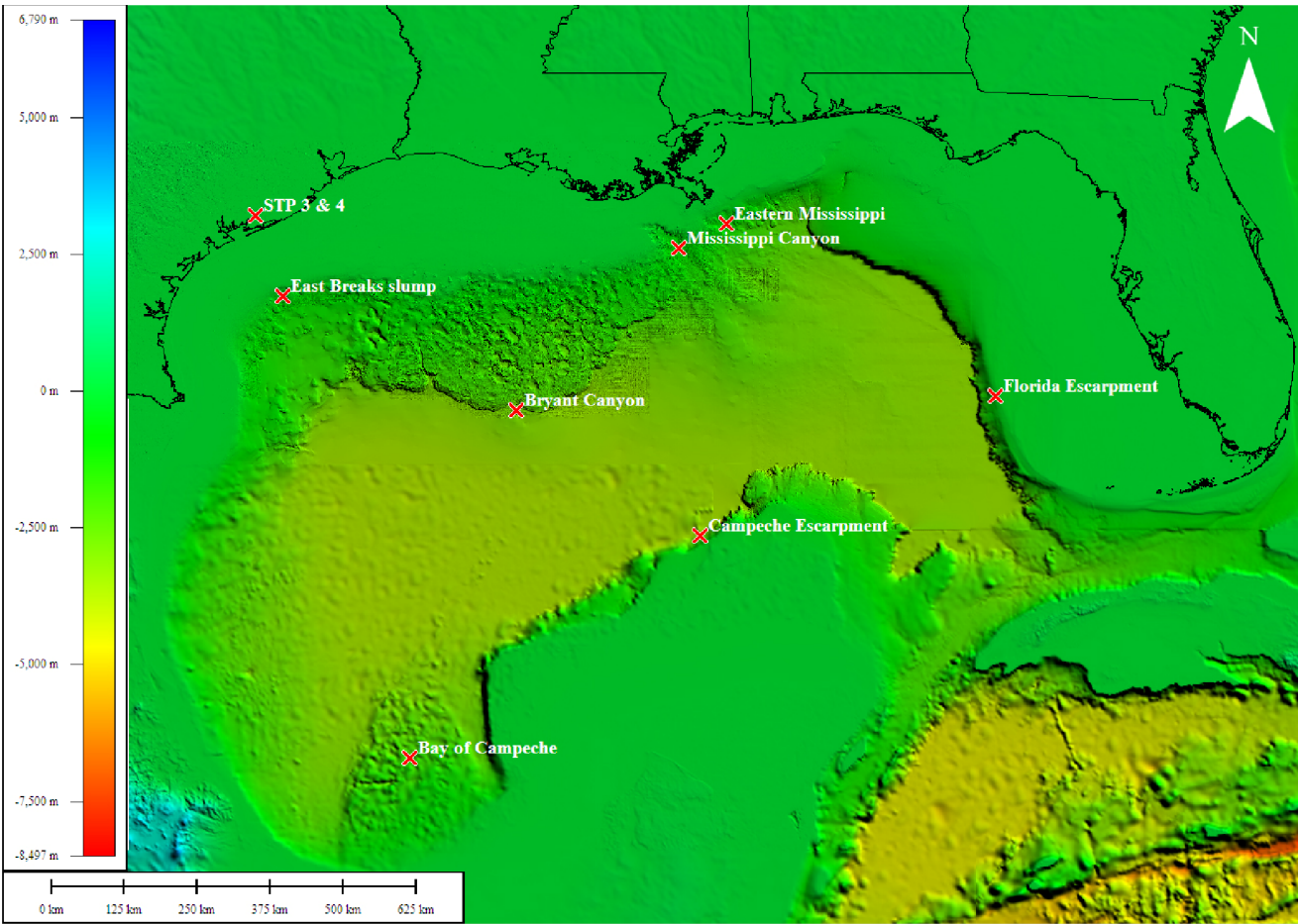
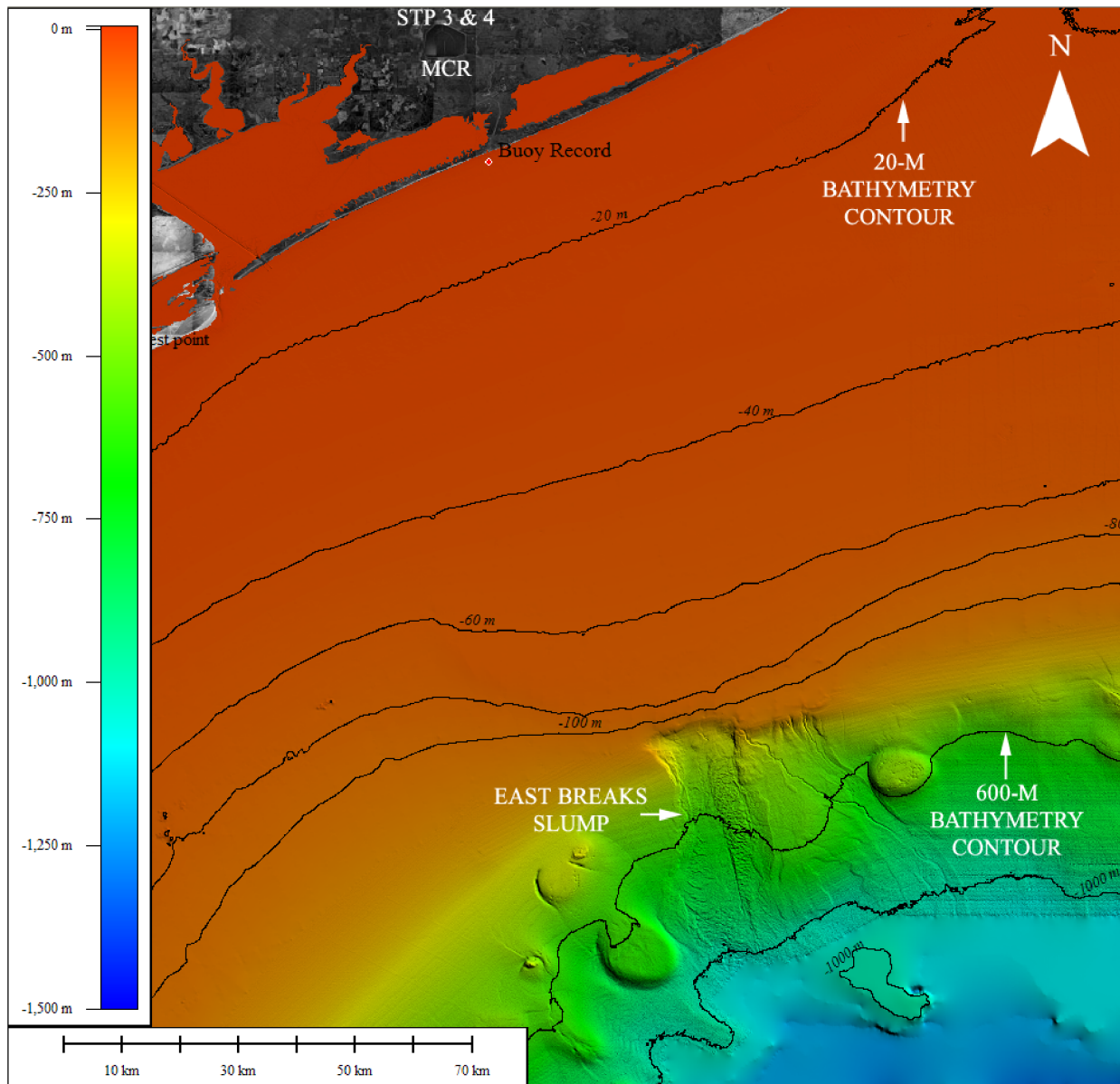


Figure 2.4S.6-2 Regional Map of Plate Boundaries and Tsunami-Generating Earthquakes from 1530-1991 in the Caribbean Sea (modified from Reference 2.4S.6-21).



**Figure 2.4S.6-3 Landslide source regions in Gulf of Mexico. At 142 km from STP 3 & 4, the East Breaks slump is the only near-field landslide source. Source of bathymetry: Reference 2.4S.6-41.**



**Figure 2.4S.6-4** Location of East Breaks slump relative to STP 3 & 4 (Source: Reference 2.4S.6-41). Buoy record for recording tsunami wave amplitudes is located at 28.58° N and 95.98° W. Bathymetry elevations are relative to Mean Sea Level (MSL).

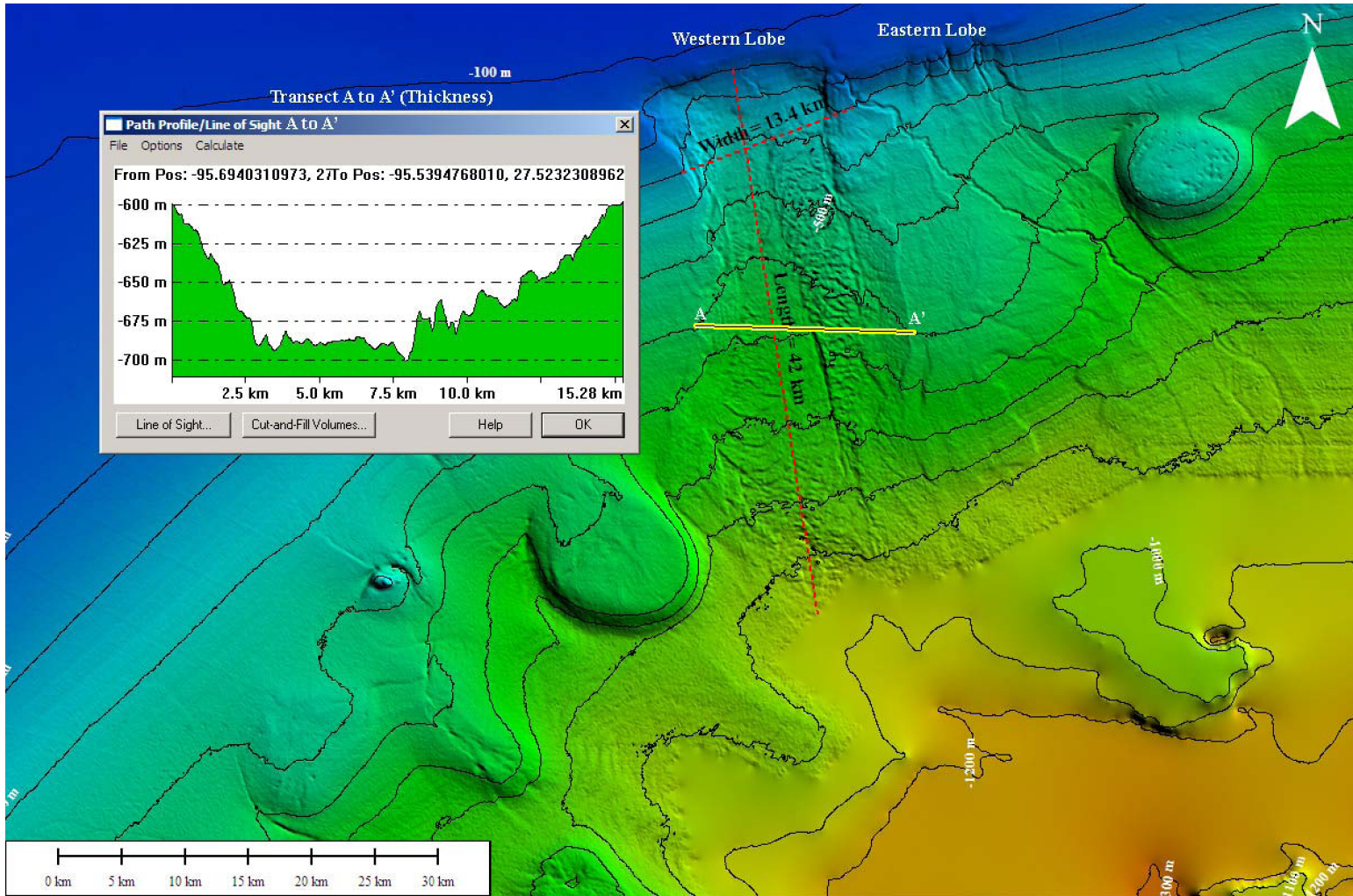


Figure 2.4S.6-5 Source parameters for East Breaks slump - Bathymetry elevations are relative to MSL. (Source of bathymetry data: Reference 2.4S.6-41)

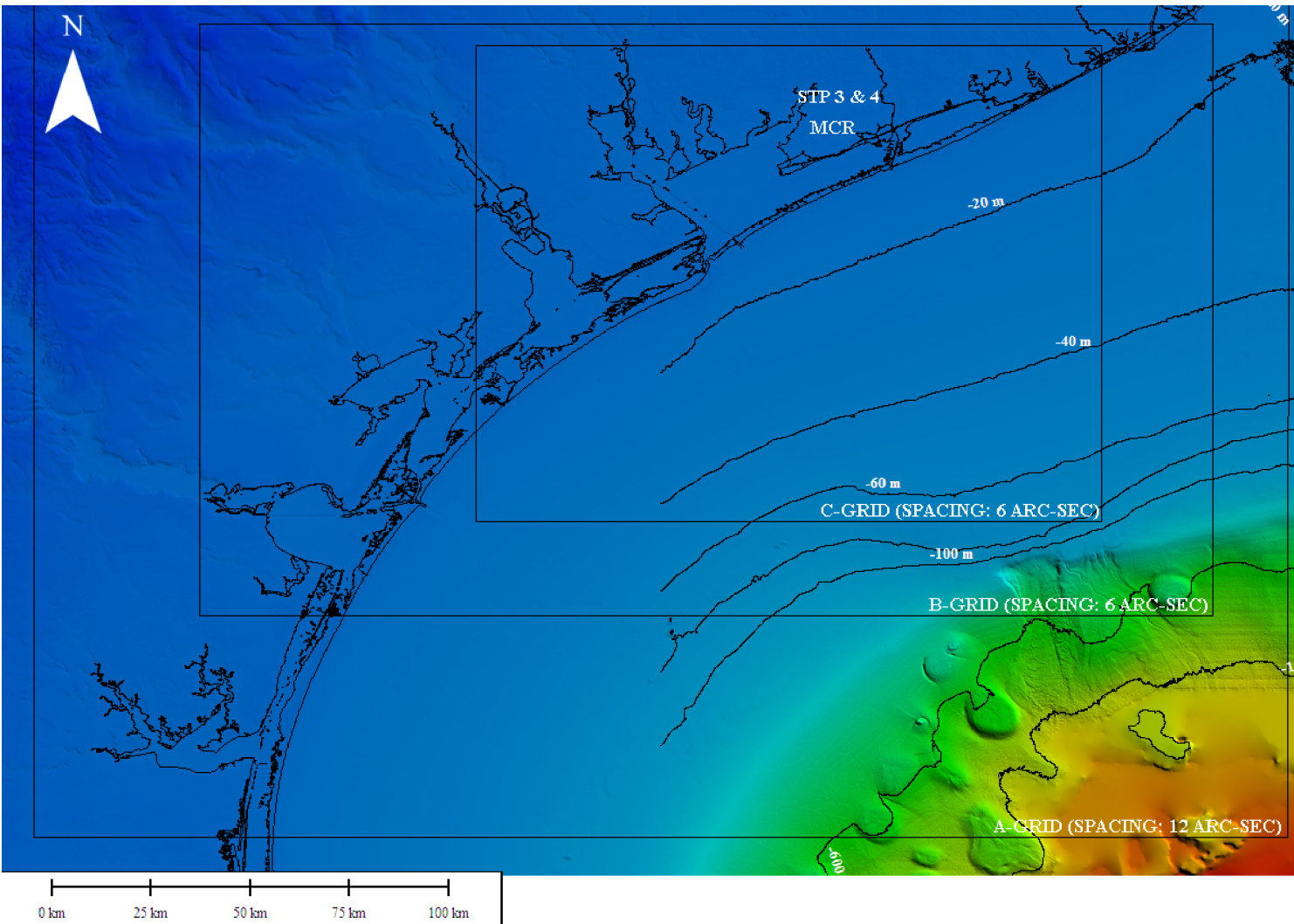
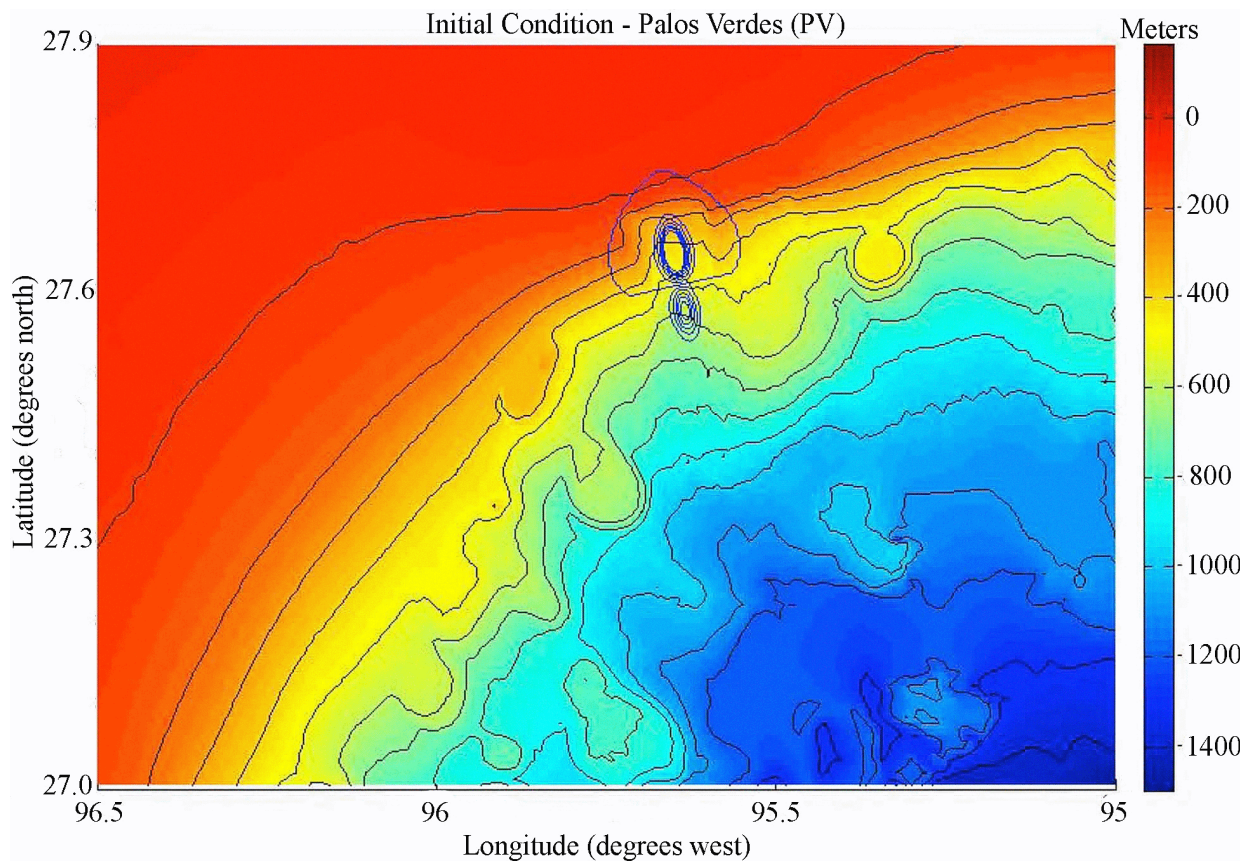
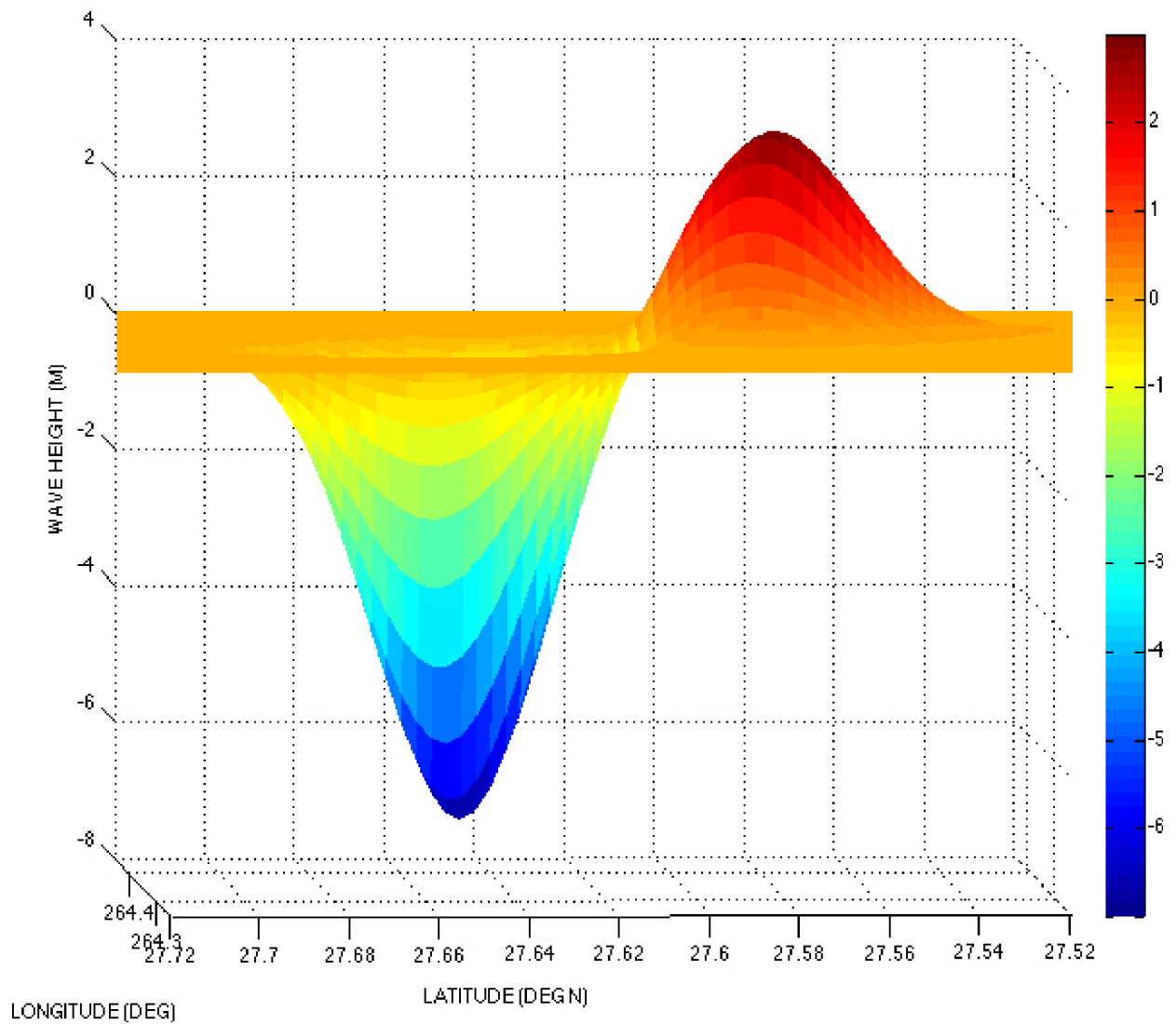


Figure 2.4S.6-6 Grid spacing for East Breaks slump modeling with MOST. Bathymetry elevations are relative to MSL. (Source of bathymetry data: Reference 2.4S.6-41)



**Figure 2.4S.6-7 Plan view of Palos Verdes (PV) initial deformation condition at location of the East Breaks slump in the Gulf of Mexico. Elevations of initial wave correspond with elevations in Figure 2.4S.6-8.**



**Figure 2.4S.6-8 Side view of Palos Verdes (PV) initial deformation condition. Maximum elevation of negative wave is -7 m (MSL); maximum elevation of positive wave is +3 m. (MSL).**

Source: Reference 2.4S.6-5, p. 5

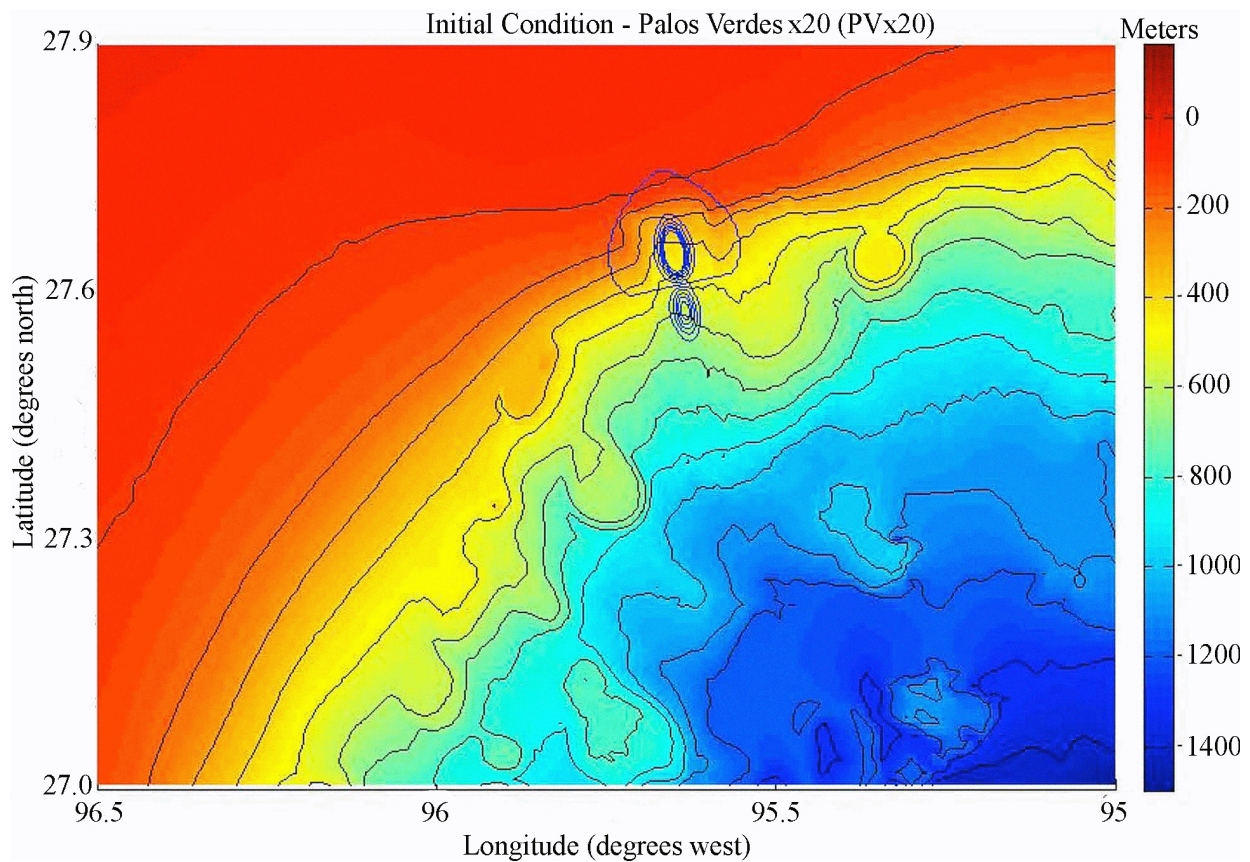


**Figure 2.4S.6-9 Plan view of Palos Verdes x20 (PVx20) initial deformation condition at location of the East Breaks slump in the Gulf of Mexico. Elevations of initial wave correspond with elevations in Figure 2.4S.6-10.**

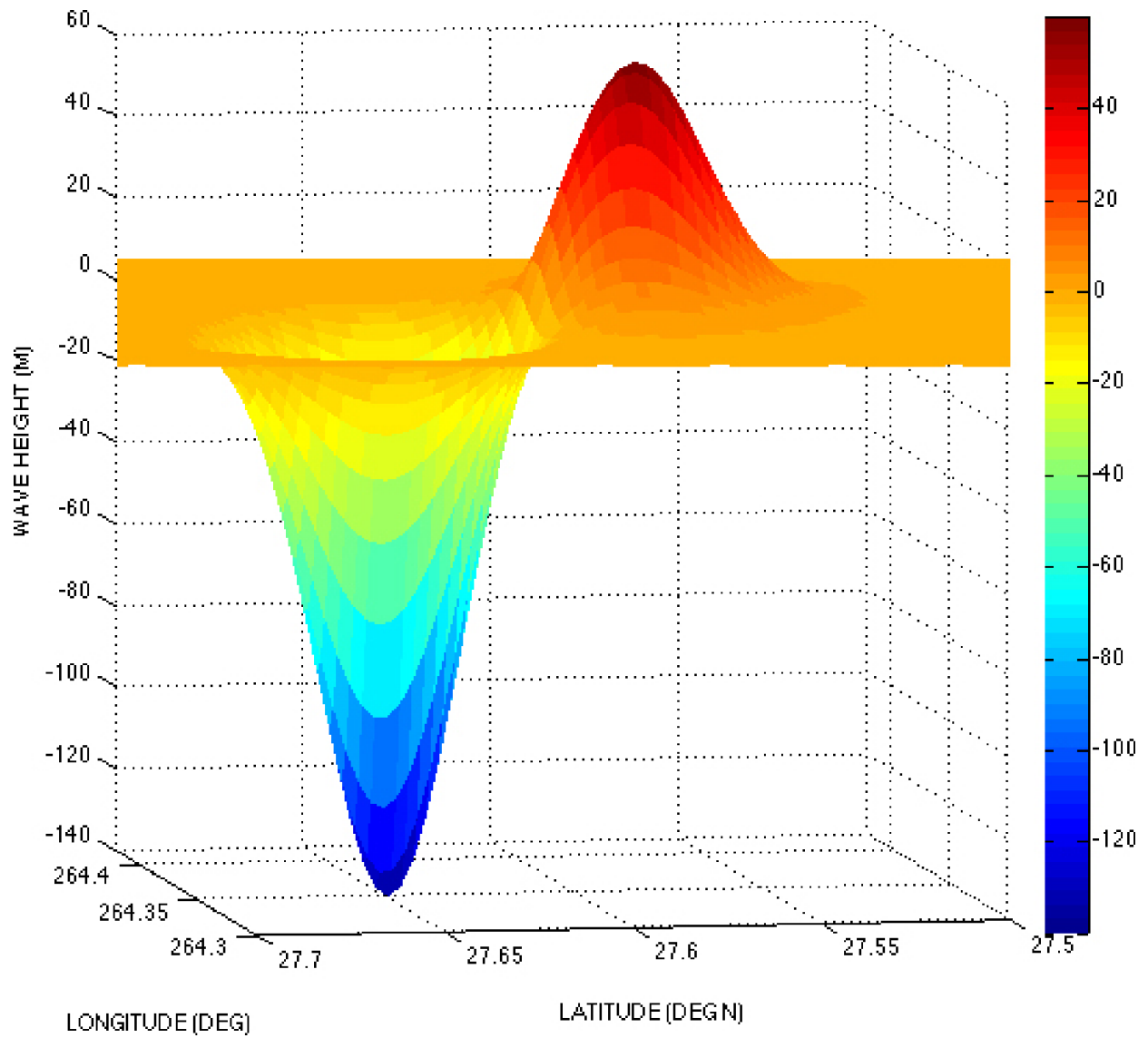


**Figure 2.4S.6-10 Side view of Palos Verdes x20 (PVx20) initial deformation condition. Maximum elevation of negative wave is -140 m (MSL); maximum elevation of positive wave is +60 m (MSL).**

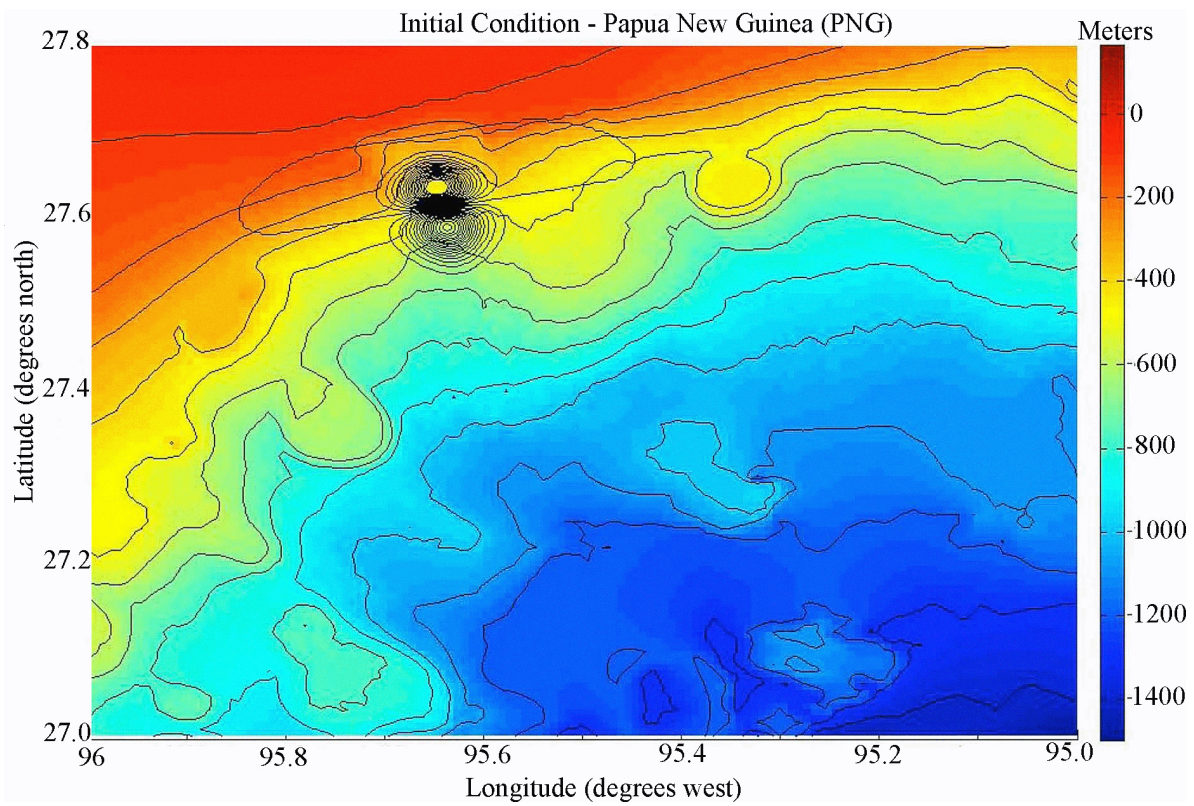


**Figure 2.4S.6-11 Plan view of Papua New Guinea (PNG) initial deformation condition at location of the East Breaks slump in the Gulf of Mexico. Elevations of initial wave correspond with elevations in Figure 2.4S.6-12.**

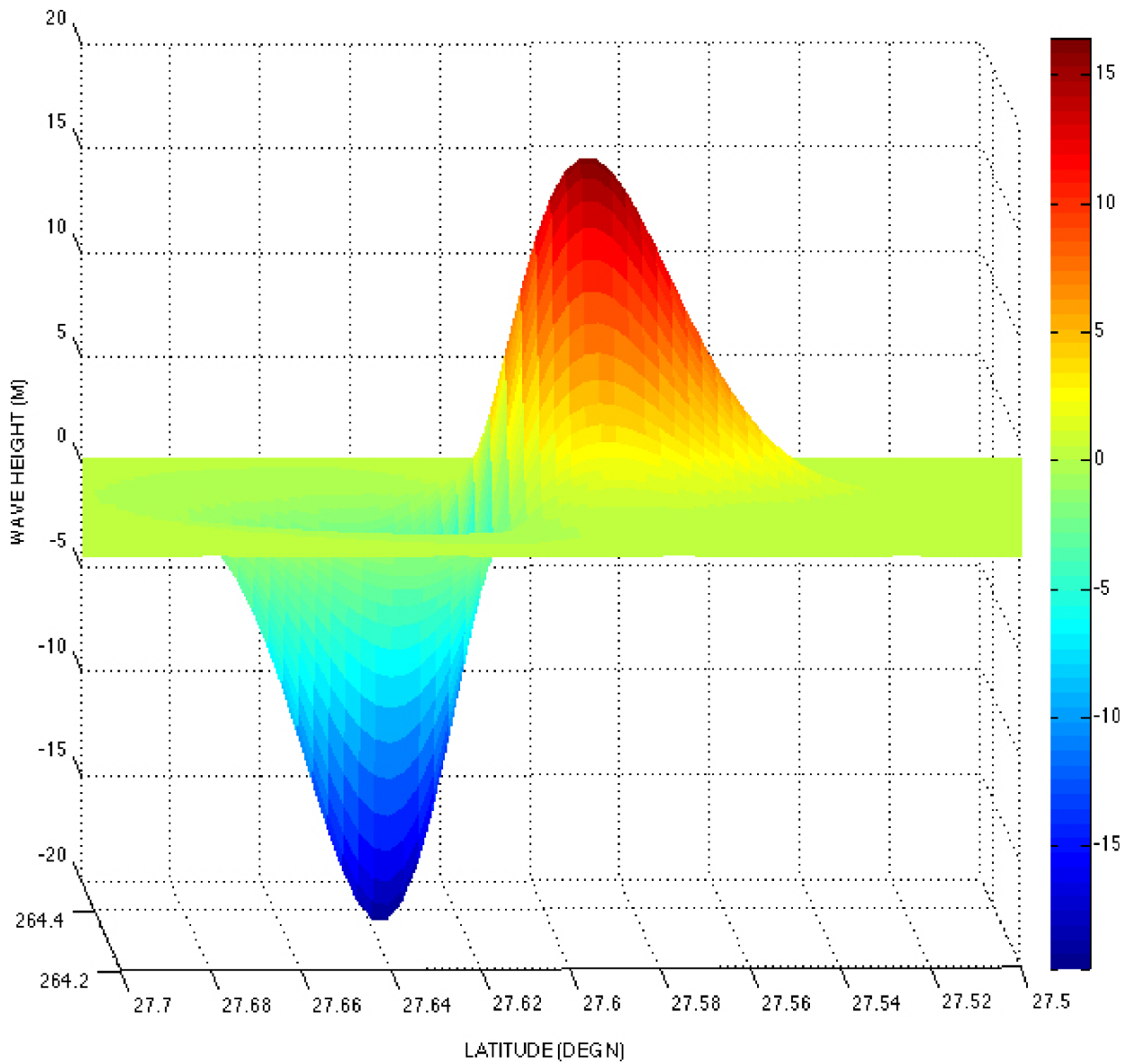


**Figure 2.4S.6-12 Plan view of Papua New Guinea (PNG) initial deformation condition. Maximum elevation of negative wave is -18 m (MSL); maximum elevation of positive wave is +16 m (MSL).**

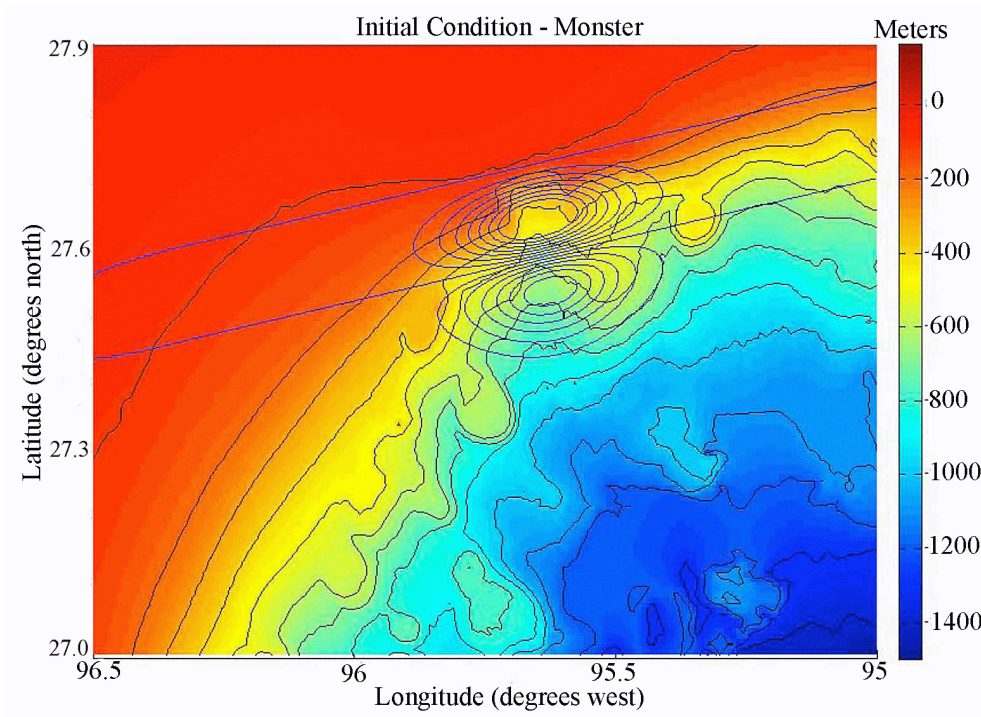


**Figure 2.4S.6-13 Plan view of hypothetical “Monster” initial deformation condition at location of the East Breaks slump in the Gulf of Mexico. Elevations of initial wave correspond with elevations in Figure 2.4S.6-14.**

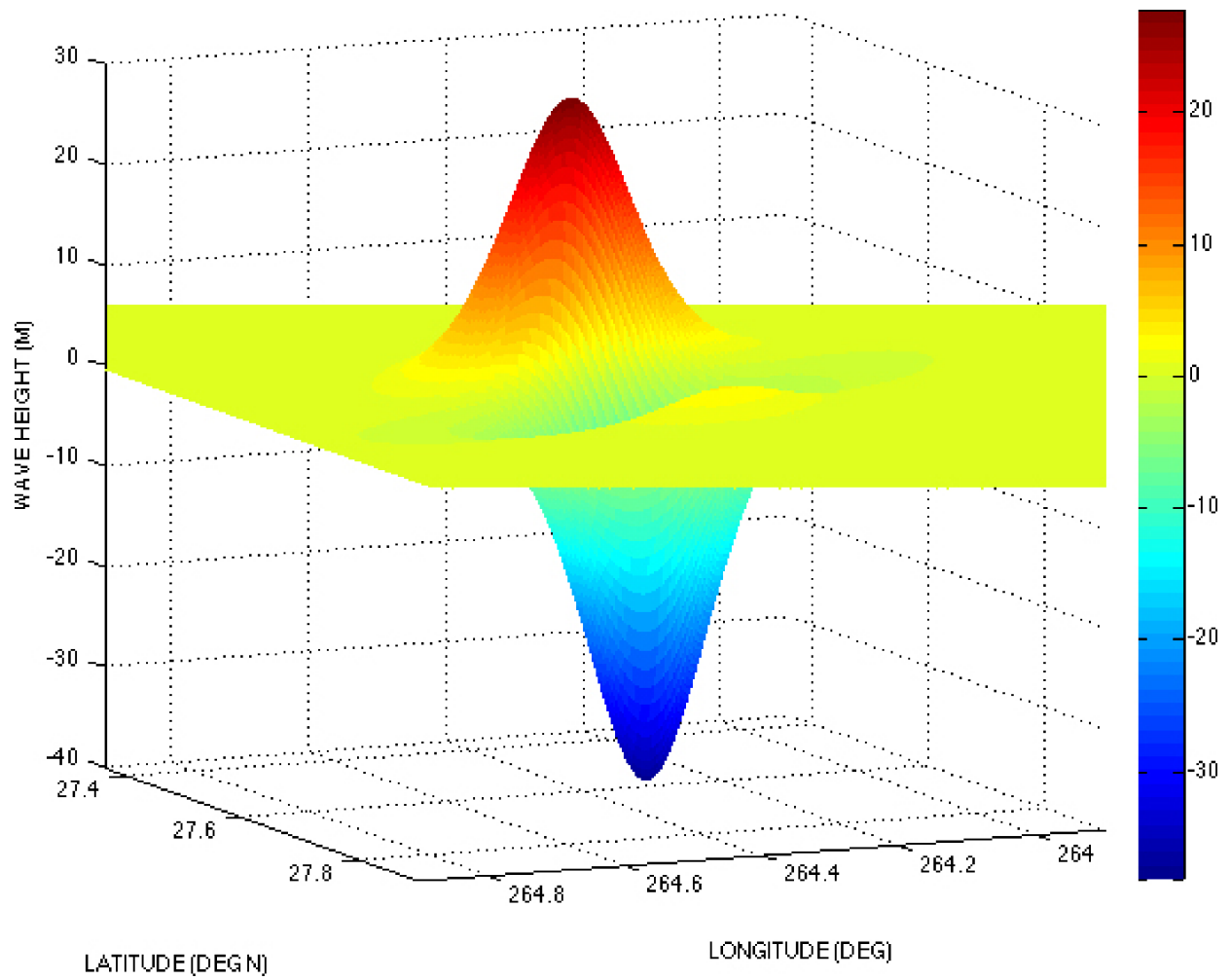


**Figure 2.4S.6-14 Oblique view of hypothetical “Monster” initial deformation condition. Maximum elevation of negative wave is -38 m (MSL); maximum elevation of positive wave is +28 m (MSL).**

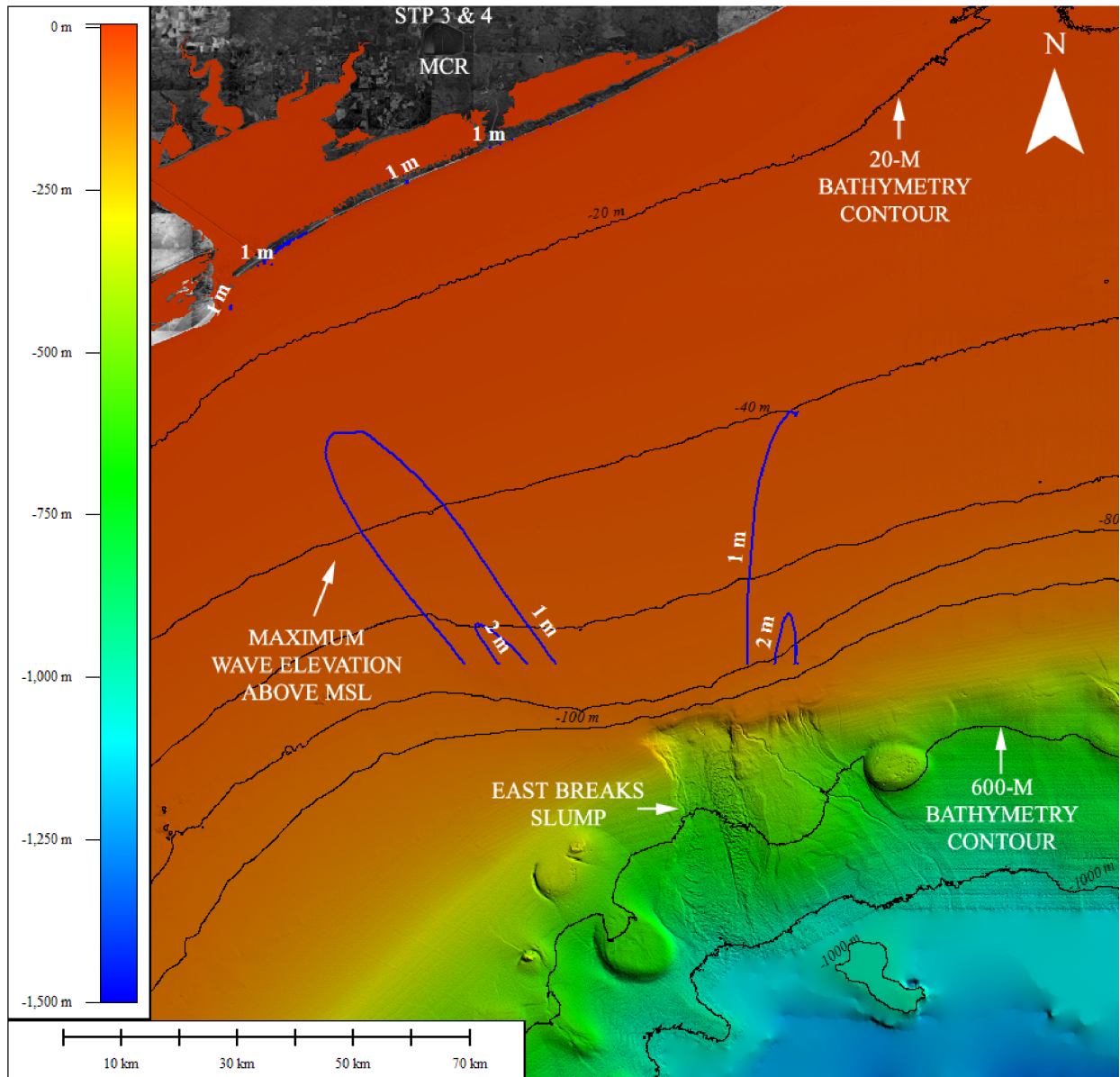
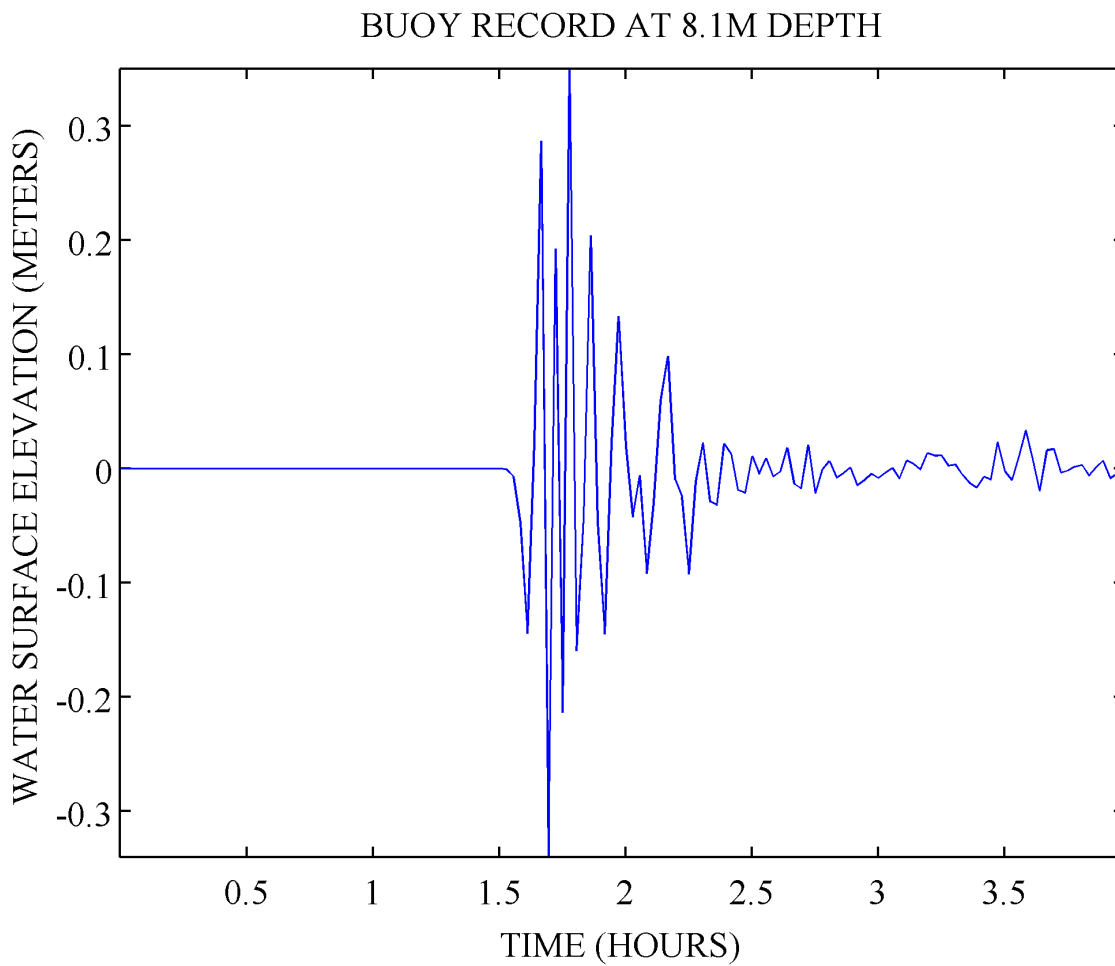


Figure 2.4S.6-15 Maximum coastal runup for the PV simulation was 1 m.



**Figure 2.4S.6-16** Time series of wave amplitude for PV simulation at 28.58° N and 95.98° W (i.e., buoy location shown in Figure 2.4S.6-4). Datum referenced to MSL.

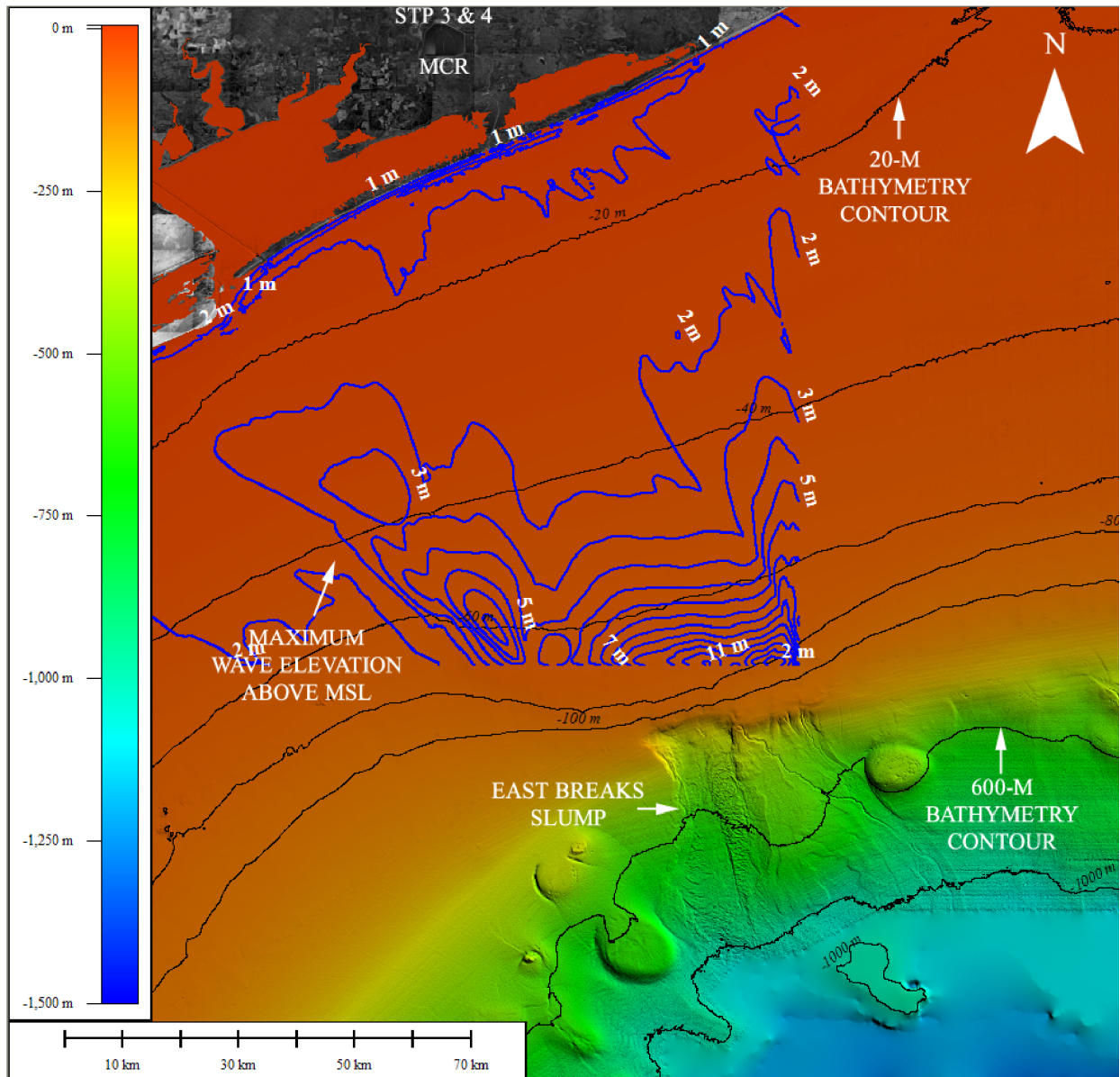
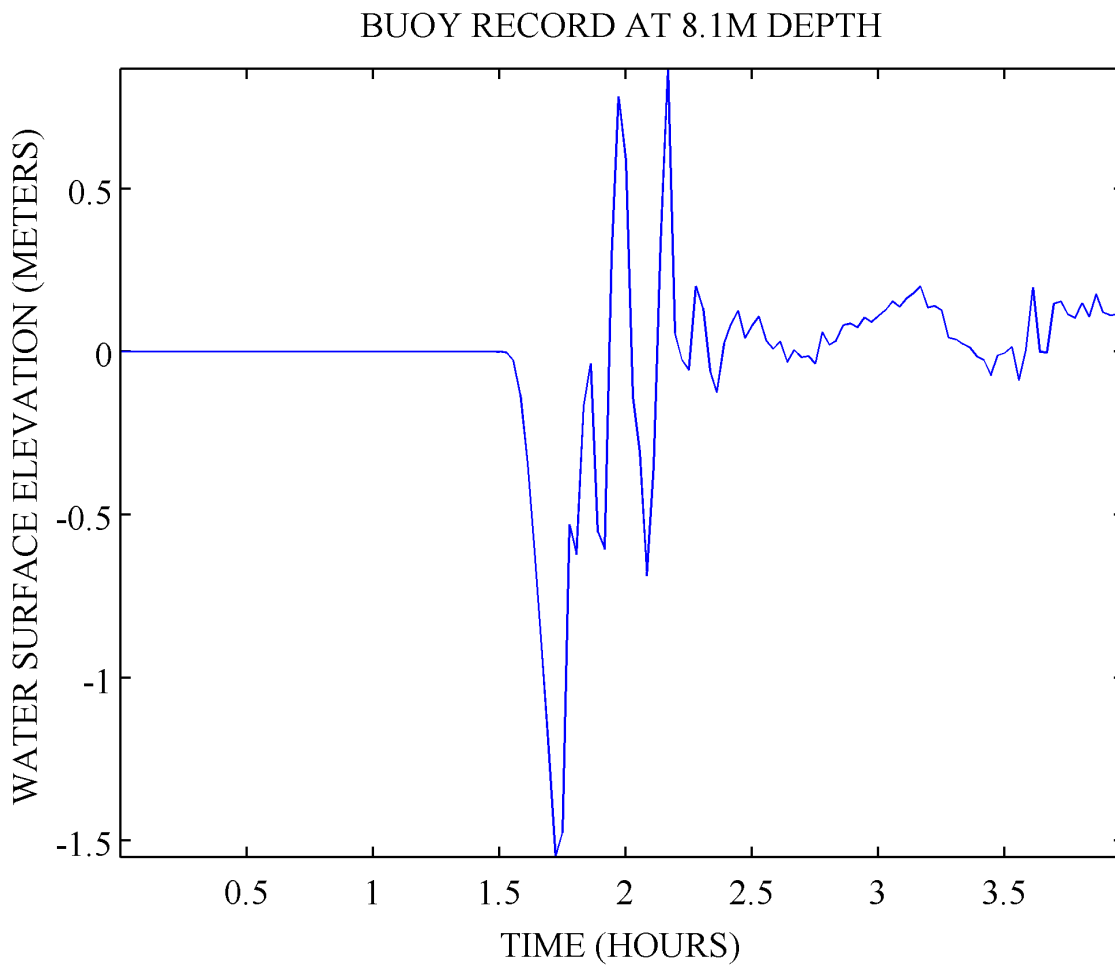


Figure 2.4S.6-17 Maximum coastal runup for the PVx20 simulation was 2 m.



**Figure 2.4S.6-18** Time series of wave amplitude for PVx20 simulation at 28.58° N and 95.98° W (i.e., buoy location shown in Figure 2.4S.6-4). Datum referenced to MSL.

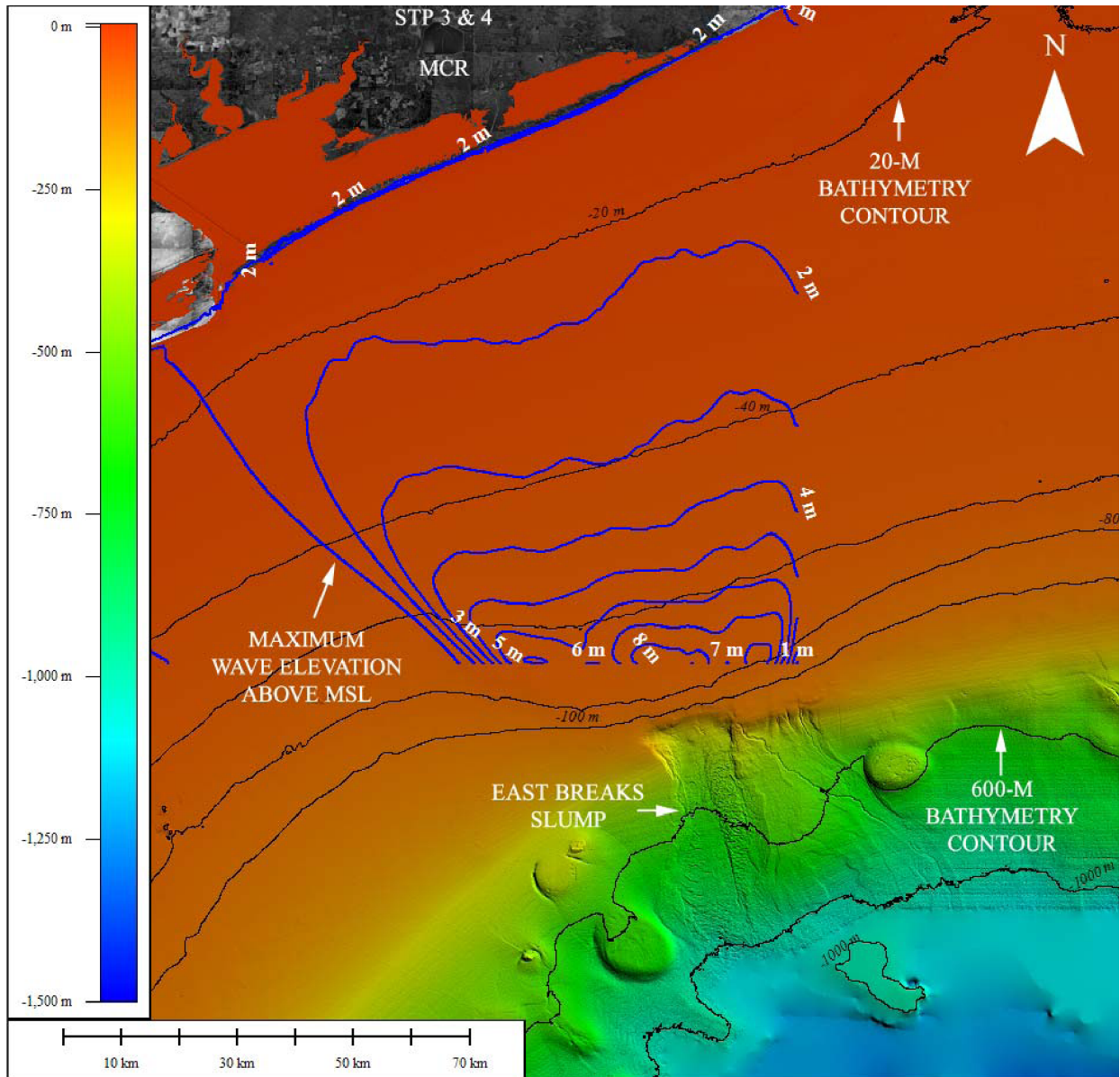
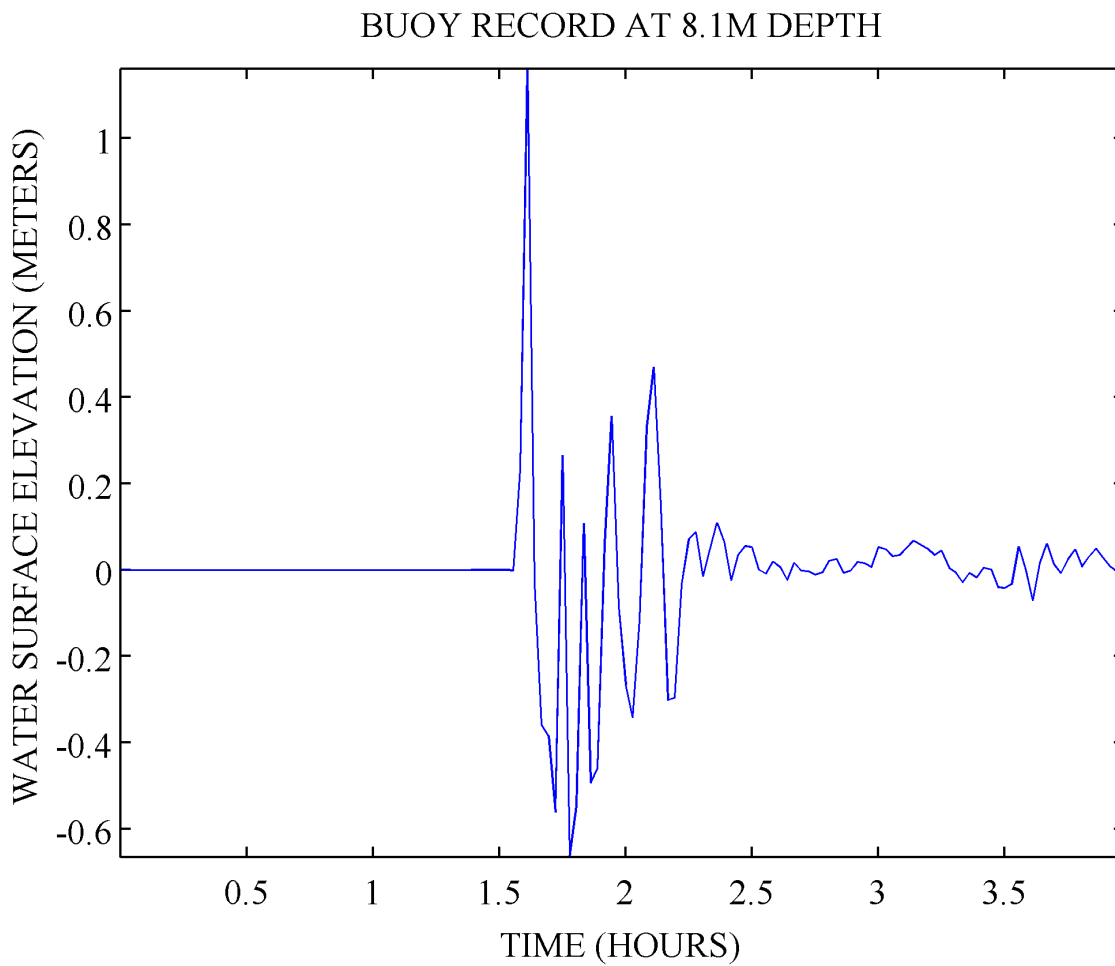


Figure 2.4S.6-19 Maximum coastal runup for the PNG simulation was 2 m.



**Figure 2.4S.6-20 Time series of wave amplitude for PNG simulation at 28.58° N and 95.98° W (i.e., buoy location shown in Figure 2.4S.6-4). Datum referenced to MSL.**

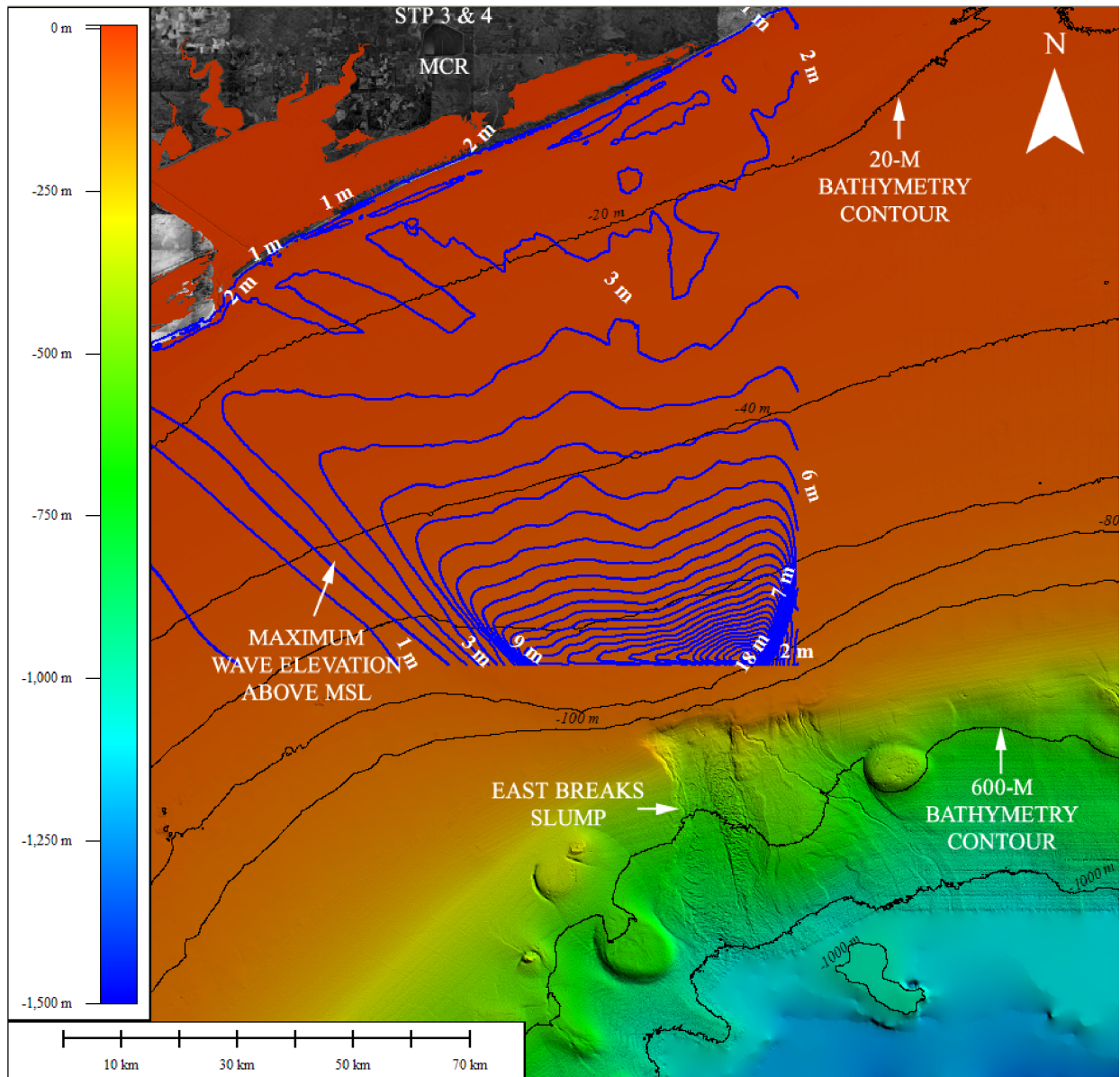
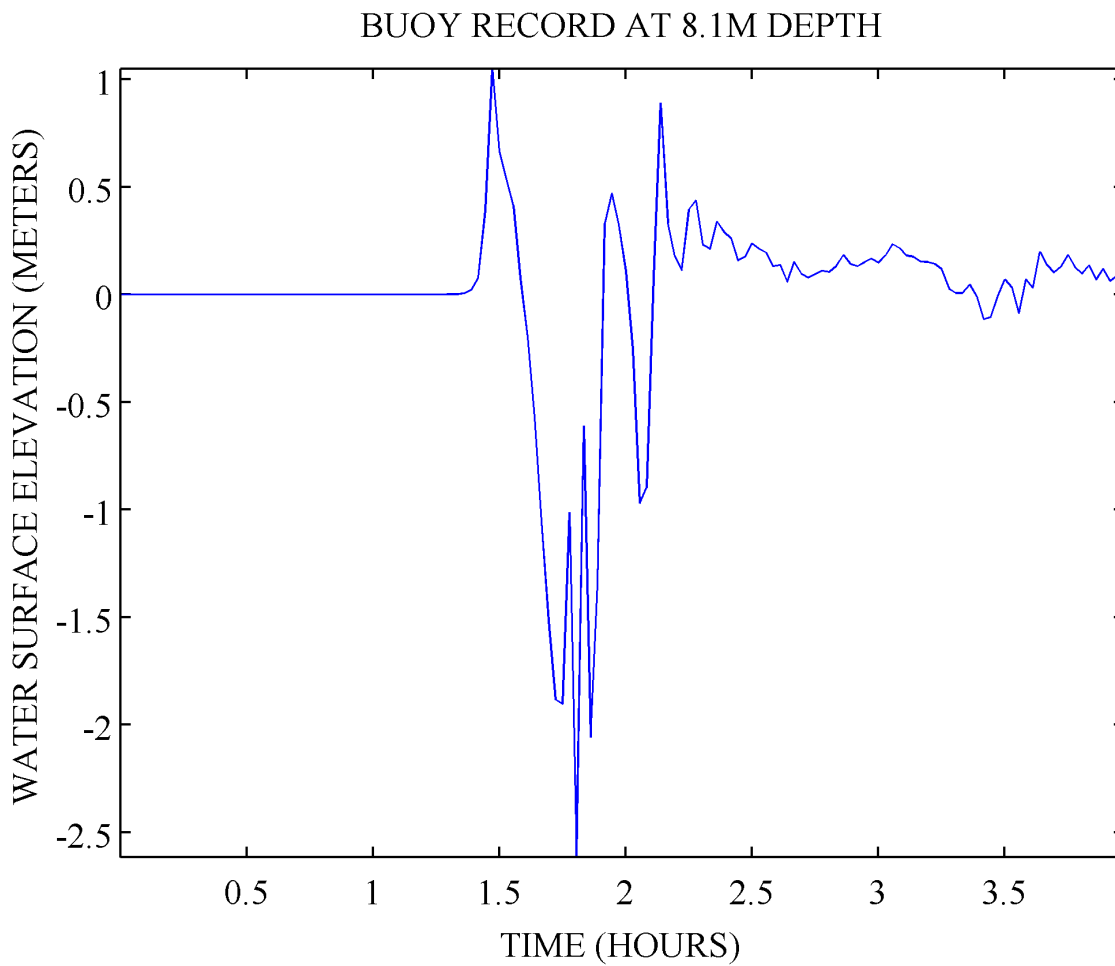


Figure 2.4S.6-21 Maximum coastal runup for the hypothetical “Monster” simulation was 2 m.



**Figure 2.4S.6-22 Time series of wave amplitude for hypothetical “Monster” simulation at 28.58° N and 95.98° W (i.e., buoy location shown in Figure 2.4S.6-4). Datum referenced to MSL.**

### 2.4S.6 ~~Probable Maximum Tsunami~~

~~The following site-specific supplement addresses the probable maximum tsunami. Probable maximum tsunami flooding events are discussed in Subsection 2.4S.2.~~

#### 2.4S.6.1 ~~Probable Maximum Tsunami~~

~~Previous estimates of “worst case” tsunami flooding along the Texas Gulf Coast have been made for near field and far field (i.e., a tsunami that occurs from a source over a 1000 km away) sources. These previous estimates have been based on both historical tsunamis and simulated events. With respect to near field sources, the National Oceanic and Atmospheric Administration’s (NOAA) West Coast and Alaska Tsunami Warning Center has estimated “worst case” events by using a two-dimensional depth-integrated hydrodynamic model developed at the University of Alaska, Fairbanks (Reference 2.4S.6-1). The model was run on a Cray X1 supercomputer and included four “worst case” scenarios based on geoseismic events originating in the Caribbean Sea and the Gulf of Mexico:~~

- ~~(1) A moment magnitude ( $M_w$ ) 9.0 in the Puerto Rico trench (66W, 18N)~~
- ~~(2) A  $M_w$  8.2 in the Caribbean Sea (85W, 21N)~~
- ~~(3) A  $M_w$  9.0 in the North Panama Deformed Belt (66W, 12N)~~
- ~~(4) A hypothetical scenario off the coast of Veracruz, Mexico (95W, 20N)~~

~~For all near field modeled scenarios, the peak shoreline wave height along the Gulf coast was less than 0.35 meters. The peak shoreline wave height for the first scenario in the vicinity of STP 3 & 4 was predicted as being between 0.04 meters and 0.06 meters (Figure 2.4S.6-1). The peak shoreline wave height for the second scenario in the vicinity of STP 3 & 4 was less than 0.1 meter (Figure 2.4S.6-2). The peak shoreline wave height for the third scenario in the vicinity of STP 3 & 4 was less than 0.06 meters (Figure 2.4S.6-2). The peak shoreline wave height for the fourth scenario in the vicinity of STP 3 & 4 was less than 0.35 meters (Figure 2.4S.6-3).~~

~~However, an extensive literature review of historical accounts, tsunami databases, and model postulations indicates the probable maximum tsunami wave height in the Gulf of Mexico is expected to occur from a far field source. The magnitude of the tsunami is expected to be no more than 1 meter. The tsunamigenic source for such a tsunami wave would be a seismic event similar to the 1755 Lisbon earthquake (Reference 2.4S.6-2).~~

~~With respect to other tsunamigenic sources, the 1 m to 2 m seiche event along the Texas coast from the 1964 Alaska earthquake (References 2.4S.6-3 and 2.4S.6-4) is considered to approximate the maximum possible seismic seiche event.~~

~~With respect to submarine landslides and slumps, the 7.6 meter wave height estimated to have been generated by the East Breaks slump (Reference 2.4S.6-5) is not considered probable. It is noted that an extensive literature search did not reveal any information or data regarding any potential submarine areas in the Gulf of Mexico of-~~

~~the size of the East Breaks slump that are considered to have a probable risk for sliding. Additional slides or slumps producing tsunamis have also not been documented for the period after this event occurred. Therefore, a tsunami along the Texas Coast of the magnitude estimated to have been generated by the East Breaks slump is considered highly unlikely and is not a consideration for STP 3 & 4.~~

#### **2.4S.6.2 Historical Tsunami Record**

~~Sources of information and data on tsunami-generating earthquakes and runup events affecting the Gulf coast include primarily the National Geophysical Data Center (NGDC) tsunami database, Science of Tsunami Hazards journal archives, the United States Geological Survey (USGS), the National Oceanic and Atmospheric Administration (NOAA) Center for Tsunami Research and published literatures on historical Caribbean tsunamis. The NGDC database contains information on source events and runup elevations for worldwide tsunamis from about 2000 B.C.E. to the present (Reference 2.4S.6-6). Similarly, the archives of the Science of Tsunami Hazards journal include source events and runup elevations for the Caribbean Sea and Eastern United States from 1498 to 1997 (Reference 2.4S.6-7) and 1668 to 1998 (Reference 2.4S.6-8). The USGS has published a fact sheet on improving earthquake and tsunami warnings for the Caribbean Sea, the Gulf of Mexico, and the Atlantic coast (Reference 2.4S.6-9) that includes a map showing the locations of the tsunami-generating earthquakes in the Caribbean Sea and Gulf of Mexico from 1530 to 1991. The map is reproduced in Figure 2.4S.6-4, which shows the locations of these tsunami-generating earthquakes and the plate boundaries in this area. NOAA's Center for Tsunami Research, in conjunction with the Pacific Marine Environmental Laboratory, has developed a database that includes worldwide event monitoring and numerical model simulations. NOAA's database includes recent tsunami events (Reference 2.4S.6-10). Finally, the publication titled "Caribbean Tsunamis: A 500 Year History from 1498-1998," is a compendium of data and anecdotal material on tsunamis reported in the Caribbean from 1498 to 1997 (Reference 2.4S.6-11).~~

~~Three historical tsunamis have been documented for the Gulf coast in the available tsunami databases and literature referenced above. The first of these tsunami events occurred on October 24, 1918. This tsunami was presumed to be an aftershock of the  $M_w=7.3$  October 11, 1918 earthquake near Puerto Rico (Reference 2.4S.6-7, p. 73). The epicenter of the earthquake was reported at 18.5°N, 67.5°W (Reference 2.4S.6-11, p. 201), which is approximately nine miles northwest of Puerto Rico in the Mona Rift. As described in Reference 2.4S.6-11 (p. 201), this earthquake was "considered a terrific aftershock of the October 11 event, both this and another earthquake on November 12 had epicentral intensities of R-F [Rossi-Forel scale] equal to approximately VIII to IX. In marked contrast to the vertical vibrations of the initial disturbance, these were characterized by horizontal oscillations. A small wave was recorded at the Galveston, Texas, tide gauge." This event has a validity rating in the NGDC database of four on a scale from zero to four, where zero and one are used for erroneous or very doubtful events, respectively, and four is used for definite events. The magnitude of the runup of this tsunami was not reported.~~

The second documented tsunami event in the Gulf occurred on May 2, 1922. The epicenter of the earthquake associated with this event was reported at 18.4°N, 64.9°W (Reference 2.4S.6-11, p. 201). Reference 2.4S.6-11 (p. 201) states that “a wave with an amplitude of 64 cm was reported on a tide gauge at Galveston. A train of three waves with a 45-minute period was followed in 8 hours by a 28-cm wave in a similar train of smaller waves. Parker (Reference 2.4S.6-12) associated it with an earthquake felt 4 hours earlier at Vieques, Puerto Rico. According to Campbell (Reference 2.4S.6-13), the two-second shock was slight and unlikely to have been the tsunamigenic source.” The validity rating of this event in the NGDC database is a two (i.e., doubtful). No runups were documented along the Gulf coast for the primary shock of the 1922 earthquake, and the surge was presumed to have been locally amplified by the inland position of the tidal gauge (Reference 2.4S.6-12, p. 30). The magnitude of the 1922 earthquake and the aftershock has not been estimated.

The third reported tsunami event in the Gulf occurred on March 27, 1964, and was recorded on a tide gauge in Freeport, Texas (Reference 2.4S.6-3). While the validity of this event was a four, estimates of the wave height vary considerably between eyewitness accounts and tide gauge data. Reference 2.4S.6-3 (p. 261) notes that “in several reports from eyewitnesses in the coastal regions of Louisiana and Texas, waves up to 6 feet (2 meters) in height were observed.” However, Reference 2.4S.6-3 (p. 261) reports that the “maximum height of the recorded seiche at 0400 GMT is about seven inches (18 cm),” and that the “true wave height may have been several feet (about a meter).” This event coincided with the 1964 Alaska ( $M_w=9.2$ ) earthquake located between the Aleutian Trench and the Aleutian Volcanic Arc (Reference 2.4S.6-14). Additional analyses of tide gauge records from the 1964 event report the maximum measured height of the low-frequency waves along the Texas coast coinciding with the Alaska earthquake ranged from 0.22 to 0.84 feet (Reference 2.4S.6-4, p. 26).

In addition to the recorded events in the Gulf of Mexico, numerical simulations of tsunamis generated by historic earthquakes provide additional insight into the potential tsunami hazards along the Texas coast. Wave generation and propagation modeling of the tsunami generated by the 1755 Lisbon ( $M_w=8.7$ ) earthquake (Reference 2.4S.6-15) was conducted using the nonlinear long wave equations and a 10-minute Mercator grid for the Atlantic Ocean (Reference 2.4S.6-2). The modeling predicted a teletsunami (i.e., a tsunami from a source over 1000 km away) arriving in the Caribbean and entering the Gulf of Mexico. Reference 2.4S.6-2 (p. 95) states that “the east coast of the U.S.A. and the Caribbean [would] receive a tsunami wave offshore in deep water about two meters high with periods of 1.25 to 1.5 hours. Such a wave would give waves along the shore about 10 feet high with Saba being unique with about a 20-foot high wave after run-up. After the wave travels into the Gulf of Mexico the wave amplitudes are less than one meter.” Saba is an island in the Netherlands Antilles located off the north coast of Venezuela. The estimate of the Saba runup elevation in Reference 2.4S.6-2 agrees well with the reported runup in Saba of 7.0 meters (Reference 2.4S.6-7, p. 78), and provides verification of the numerical model, even for unique situations such as Saba.

### 2.4S.6.3 ~~Source-Generator Characteristics~~

~~Several tsunamigenic sources have been documented for the Gulf of Mexico and the Texas-Louisiana coast. These sources include seismic events in the Azores-Gibraltar fracture zone near Lisbon, Portugal, seismic events in the North Caribbean, seiche mechanisms associated with earthquakes in other parts of the world (e.g., the large Alaskan earthquakes), volcanism in the Atlantic Ocean (e.g., in the Canary Islands). While submarine landslides and submarine slumps causing tsunamis have not been documented in historical times, at least one event has been conjectured to have occurred within the Gulf of Mexico within the last 5,000 to 10,000 years. These tsunamigenic sources are discussed in further details below.~~

#### 2.4S.6.3.1 ~~Seismic tsunamis~~

~~In comparison to islands in the Caribbean, the Gulf of Mexico and the Texas coast has had relatively few seismic tsunamis. Reference 2.4S.6-1 (p. 311) states that “the Atlantic and Gulf coasts are nearly independent since the hydrodynamic connection between basins is through the narrow Straits of Florida and through the Caribbean, where bottom friction losses appear to be large.” As discussed in Reference 2.4S.6-1 (p. 307), wave propagation takes two routes, “one through the Caribbean and the other through the Straits of Florida.” The Caribbean route is faster by about one hour, and energy transfer into the Gulf is computed with an energy flux vector that is a function of the wave momentum and kinetic energy. While wave propagation is faster through the Caribbean than the Straits of Florida, energy dissipation is larger in the Caribbean Sea than in the Straits of Florida (Figure 2.4S.6-5). Consequently, although the wave arrives later, more energy moves into the Gulf through the Straits of Florida. Reference 2.4S.6-1 (p. 311) therefore concluded that “sources outside the Gulf are not expected to create a tsunami threatening to the Gulf coast.”~~

#### 2.4S.6.3.2 ~~Seismic seiches~~

~~The only documented event that has produced a seismic seiche in the Texas coast is the 1964 Alaska earthquake. Reference 2.4S.6-4 indicated that the horizontal acceleration associated with the seismic surface waves from the Alaska shock appears to have varied markedly within North America according to data from seiches recorded by surface water gages at the time of the Alaska shock. The amplitude of horizontal acceleration was especially large along the Gulf coast. Reference 2.4S.6-4 (p. 27) further stated that “the thick deposits of sediments of low rigidity along the Gulf coast, for example, are capable of amplifying the horizontal acceleration of surface waves to a considerable extent; this accounts for the concentration of seiches that occurred along the Gulf coast.”~~

~~While the  $M_w=9.5$  magnitude 1960 earthquake in Chile might also have been expected to have caused seiches along the Texas coast, tide gauges along the Gulf coast did not record any such event. The  $M_w=7.8$  New Madrid earthquake occurred on February 7, 1812 (Reference 2.4S.6-16), which is the largest earthquake recorded in the contiguous United States, produced significant seiches in the Mississippi River and in waterways along the Texas state boundary (Reference 2.4S.6-8, p. 124). However, no records exist to indicate that the 1812 New Madrid earthquake directly affected the Texas coast or the Lower Colorado River in the vicinity of STP 3 & 4.~~

### 2.4S.6.3.3 ~~Volcanism-based tsunamis~~

~~While volcanism and volcanism-based tsunamis have been significant in the Caribbean and Canary Islands (Reference 2.4S.6-17), no tsunamis have been documented in the Gulf of Mexico as a result of recent volcanic eruptions or associated mass wasting events (i.e., the gravity-driven mass movement of soil, regolith, or rock downslope). The largest postulated tsunami in the Atlantic Ocean that may have been caused by a volcanic eruption is that associated with the eruption and collapse of the Cumbre Vieja Volcano on the Island of La Palma in the Canary Islands about 550,000 years before the present time (Reference 2.4S.6-17). The collapse of 500 cubic kilometers of material from Cumbre Vieja has been estimated as capable of generating a transatlantic tsunami with a wave height on the order of 10-25 meters. Reference 2.4S.6-18 (p. 38) states that "during an eruption in 1949 a fault broke surface along the crest of the volcano and part of its western side slid five meters down and toward the ocean. The volcano again may be showing initial stages of instability. However, certainly collapse is not imminent and it may take many eruptive cycles over the next few thousand years to give it that final shove." In addition, the distribution of slide blocks on the ocean bottom suggests the collapse of the Cumbre Vieja may not have been the result of a single catastrophic event, but of several smaller events. A recent report on potential tsunami threats to the UK concludes that "studies of the offshore turbidities [i.e., poorly sorted sediment that is deposited from a density flow of mixed water and sediment] created by landslides from the flanks of the Canary Islands suggest that these result from multiple landslides spread over periods of several days" and are therefore "likely to create tsunamis of only local concern" (Reference 2.4S.6-19, p. 23 and p. 30, respectively). Consequently, this mechanism is not considered further as a potential source of tsunamis along the Texas coast.~~

### 2.4S.6.3.4 ~~Submarine slump tsunamis~~

~~Recent tsunami research has differentiated tsunamis from submarine sources into two types of events: tsunamis from translational landslides and tsunamis from rotational slumps (Reference 2.4S.6-20). While translational landslides are relatively frequent in the Gulf of Mexico (Reference 2.4S.6-21), no tsunamis generated by this type of landslide have been documented in the geologic record or the instrumental record for the Gulf coast. The only evidence of a submarine slump in the Gulf of Mexico with the potential to have caused a tsunami is from a topographic scar known as the East Breaks slump that occurred in the northwestern Gulf of Mexico. The slump originated within late Wisconsinian Colorado/Brazos River shelf edge deposits estimated as early Holocene in age (i.e., 10,000 to 5000 years before the present time) (Reference 2.4S.6-5). The location of the East Breaks slump is shown in Figure 2.4S.6-6. Figure 2.4S.6-7 shows the extent of the slump. The East Breaks slump has been conjectured to have initiated in unconsolidated prodeltaic sediments, with a 20 km wide head scarp, at about the 180 m isobath. The length of the erosional chute was estimated to have been about 55 km, and the maximum thickness of the slump equal to about 70 meters. The total estimated volume of the slide was about 50 to 60 cubic kilometers.~~

~~Reference 2.4S.6-5 provides a preliminary order of magnitude estimate of the offshore wave height associated with such a slump as 7.6 meters. However, no calculation or methodology was included in the conference paper where this estimate was~~

~~presented. In addition, this wave height estimate from the East Breaks slump has not been supported by subsequent publications in any peer reviewed technical or scientific journals. In part, the lack of a credible estimate is due to a poor understanding of slump based tsunamis. For example, the first slump that has high quality runup data is the 1998 Papua New Guinea event (References 2.4S.6-8 and 2.4S.6-20). Slump tsunamis in areas with low bed slopes, such as that for the Gulf of Mexico, are very poorly understood. There is no geologic evidence that has been obtained validating a wave height of this magnitude impacting the Gulf coast. In the absence of credible evidence, it is concluded that the East Breaks slide is not a probable candidate to consider for the probable maximum tsunami (PMT) runup event for STP 3 & 4.~~

#### **2.4S.6.4 Tsunami Analysis**

~~Based on the discussion presented in Section 2.4S.6.3, and considering that no other specific information exists on potential seismic sources and submarine landslides that may cause a tsunami in the Gulf of Mexico, no further detailed modeling analysis of tsunami wave height and its propagation is warranted.~~

#### **2.4S.6.5 Tsunami Water Levels**

~~Because Caribbean based tsunamis are unlikely to produce a shoreline wave height exceeding 0.35 meter at the Texas coast near STP 3 & 4, the most likely candidate for the probable maximum tsunami is from an event similar to the 1755 earthquake in the Azores Gibraltar fracture zone near Lisbon, Portugal. As discussed in other tsunami investigations (Reference 2.4S.6-19), the 1755 Lisbon event is considered to be the 'worst case' scenario with respect to a tsunami forming in the Azores Gibraltar fracture zone.~~

~~The numerical model study described in Reference 2.4S.6-2 suggested that the 1755 Lisbon event could produce wave amplitudes of less than one meter in the Gulf of Mexico. With a runup amplification of two to three times the deep water wave amplitude (References 2.4S.6-2, p. 95 and 2.4S.6-22), a conservative estimate of the maximum tsunami runup at the Texas coast would be no more than three meters (10 feet). It should be noted that in many cases, runup elevation is often lower than the shoreline wave height (Reference 2.4S.6-23). To determine the maximum flood level for a PMT event, Regulatory Guide 1.59 (Reference 2.4S.6-24) requires the consideration of the coincidental occurrence of the 10% exceedance of the astronomical high tide and sea level anomaly in addition to the wave runup. Based on tide gauge data for Freeport, Texas, the 10% exceedance of the astronomical high tide is 2.2 feet above mean low water (MLW), and the initial rise is 2.4 feet (Reference 2.4S.6-24). To account for the long term sea level rises due to global climate change, it is assumed that the historical mean sea level trend at Freeport, Texas of 5.87 mm/year or 1.93 feet/century, with a standard error of 0.74 mm/yr, from 1954 to 1999 (Reference 2.4S.6-25) will continue. The peak flood level due to a probable maximum tsunami event is therefore estimated to be of the order of 17 feet MLW within the next century. This is equivalent to 16.3 feet MSL (or NGVD 29) considering the datum shift of 0.68 feet from MLW to MSL at Freeport, Texas (Reference 2.4S.6-25).~~

With respect to the assumption of the MSL datum (or NGVD 29) shift relative to actual mean sea level from tidal measurements, it should be noted that the Freeport, Texas, tide gauge does not have a published or official NGVD29 orthometric height mark. Since the one mark that does exist suggests the difference between MSL (or NGVD 29) to actual mean sea level is small (i.e., within  $\pm 0.2$  ft of the Mean Lower Low Water datum), the shift to MSL (or NGVD 29) should be considered as an approximation of the actual value.

Based on the discussion above, it is concluded that the flood elevation at STP 3 & 4 due to the postulated probable maximum tsunami event will not be the controlling design basis flood elevation for STP 3 & 4 because it is lower than the maximum flood elevation of 48.5 feet MSL predicted for a hypothetical breach event of the MGR embankment as described in Section 2.4S.4. Coincident wind waves are not considered in the analysis since the PMT event will have no flooding impacts on safety-related facilities of STP 3 & 4.

#### 2.4S.6.6 ~~Hydrography and Harbor or Breakwater Influences on Tsunami~~

Because STP 3 & 4 is over 15 miles inland from the Gulf coast and the grade elevations for the plant are much higher than 16.3 feet MSL, there will be no local onsite effects associated with different tsunami types, including breaking waves, bores, or any resonance effects that would result in higher tsunami runup on the safety-related facilities. Therefore, no analysis of the translation of tsunami waves from offshore generator locations to the site is warranted.

#### 2.4S.6.7 ~~Effects on Safety Related Facilities~~

The postulated maximum flood level of no more than 16.3 ft MSL due to the PMT event is lower than the nominal plant grade of 34 ft MSL and the entrance level grade elevation of 35 ft MSL for all safety-related facilities of STP 3 & 4. Therefore, the PMT event will have no flooding impacts on safety-related facilities or the design basis functions of STP 3 & 4, and there will be no impact of debris and water borne projectiles and impacts of sediment erosion and deposition on the safety-related facilities of STP 3 & 4.

#### 2.4S.6.8 ~~References~~

- 2.4S.6-1 "Model Predictions of Gulf and Southern Atlantic Coast Tsunami Impacts from a Distribution of Sources," Knight, B. 2006, Science of Tsunami Hazards 24(2): 304-312.
- 2.4S.6-2 "Modeling the 1755 Lisbon Tsunami. Science of Tsunami Hazards," 19(2): 93-95, Mader, G. M.
- 2.4S.6-3 "Alaska Earthquake of 27 March 1964: Remote Seiche Stimulation. Science 145: 261-262," Donn, W. L. 1964.

- 2.4S.6-4 ~~“Seismic Seiches in Bays, Channels, and Estuaries, from The Great Alaska Earthquake of 1964: Oceanography and Coastal Engineering,” McGarr, A. and R. C. Vorhis. 1972, National Academy of Sciences, Washington, D.C. 25-28.~~
- 2.4S.6-5 ~~“East Breaks Slump, Northwest Gulf of Mexico,” Offshore Technology Conference, OTC paper 12960, Trabant, P., Watts, P., Lettieri, F. and G. Jamieson. 2001.~~
- 2.4S.6-6 ~~“Historical Tsunami Database,” National Geophysical Data Center/World Data Center. Available at [http://www.ngdc.noaa.gov/seg/hazard/tsu\\_db.shtml](http://www.ngdc.noaa.gov/seg/hazard/tsu_db.shtml), accessed March 20, 2007.~~
- 2.4S.6-7 ~~“A Brief History of Tsunamis in the Caribbean Sea. Science of Tsunami Hazards,” 20(2): 57-94, Lander, J. F., Whiteside, L. S., and P. A. Lockridge, 2002.~~
- 2.4S.6-8 ~~“Tsunamis and Tsunami-Like Waves of the Eastern United States,” Science of Tsunami Hazards 20(3): 120-157, Lockridge, P. A., Lowell, S. W., and J. F. Lander. 2002.~~
- 2.4S.6-9 ~~“Improving Earthquake and Tsunami Warnings for the Caribbean Sea, the Gulf of Mexico, and the Atlantic Coast,” USGS Fact Sheet 2006-3012, United States Geological Survey, 2006.~~
- 2.4S.6-10 ~~“Recent and Historical Tsunami Events and Relevant Data.” National Oceanic and Atmospheric Administration Center for Tsunami Research and Pacific Marine Environmental Laboratory. Available at [http://netr.pmel.noaa.gov/database\\_devel.html](http://netr.pmel.noaa.gov/database_devel.html), accessed March 29, 2007.~~
- 2.4S.6-11 ~~“Caribbean Tsunamis: A 500 Year History from 1498-1999. Kluwer Academic Publishers,” O’Loughlin, K. F. and J. F. Lander. 2006. The Netherlands. 280 pp.~~
- 2.4S.6-12 ~~“Unusual Tide Registration of Earthquake,” Parker, W.E. 1922. Bulletin of the Seismological Society in America, pp. 28-30.~~
- 2.4S.6-13 ~~“Earthquake History of Puerto Rico, Seismicity Investigation, Appendix I, Part A, Aguirre Nuclear Power Plant, Weston Geophysical Research,” Campbell, J.B. 1991, Weston, Massachusetts.~~
- 2.4S.6-14 ~~“Historical Earthquakes, Prince William Sound, Alaska,” United States Geological Survey, Available at [http://earthquake.usgs.gov/regional/states/events/1964\\_03\\_28.php](http://earthquake.usgs.gov/regional/states/events/1964_03_28.php), accessed April 27, 2007.~~

- 2.4S.6-15 ~~United States Geological Survey, Historical Earthquakes, Lisbon, Portugal. Available at [http://earthquake.usgs.gov/regional/states/events/1964\\_03\\_28.php](http://earthquake.usgs.gov/regional/states/events/1964_03_28.php), accessed April 27, 2007.~~
- 2.4S.6-16 ~~"Magnitudes and locations of the 1811-1812 New Madrid, Missouri, and the 1886 Charleston, South Carolina, Earthquakes," Bakun, W. H. and M. G. Hopper. 2004. Bulletin of the Seismological Society of America 94(1): 64-75.~~
- 2.4S.6-17 ~~"Cumbre Vieja Volcano—Potential Collapse and Tsunami at La Palma, Canary Islands," Ward, S. N. and S. Day. 2001. Geophysical Research Letters 28(17): 3397-3400.~~
- 2.4S.6-18 ~~"Tsunami Thoughts. Recorder—Journal of the Canadian Society of Exploration Geophysicists," Ward, S. N. and S. Day, 39-44, December 25, 2005.~~
- 2.4S.6-19 ~~"The Threat Posed by the Tsunami to the UK," British Geology Society, 2005. Study commissioned by Debra Flood Management, 133 pp.~~
- 2.4S.6-20 ~~"Tsunami and Seiche," Synolakis, C. E. 2004 from Earthquake Engineering Handbook, edited by Chen, W. F. and C. Scawthorn, CRC Press. 9-1 to 9-90.~~
- 2.4S.6-21 ~~McAdde, B.G., Pratson, L.E. and Orange, D.L. 2000. Submarine Landslide Geomorphology, US Continental Slope. Marine Geology 169: 103-136.~~
- 2.4S.6-22 ~~"Numerical Modeling of Water Waves," Mader, C. L. 1988. University of California Press, Berkeley, California.~~
- 2.4S.6-23 ~~"Tsunami Engineering," Camfield, F. E. 1980. Special Report No. 6. U.S. Army Coastal Engineering Research Center, Fort Belvoir, Virginia.~~
- 2.4S.6-24 ~~"Design Basis Floods for Nuclear Power Plants," U.S. Nuclear Regulatory Commission, Regulatory Guide 1.59, Revision 2, 1977.~~
- 2.4S.6-25 ~~"Tides and Currents," National Oceanic and Atmospheric Administration. Available at [http://tidesandcurrents.noaa.gov/data\\_menu.shtml?stn=8772440%20Freeport,%20TX&type=Tide%20Data](http://tidesandcurrents.noaa.gov/data_menu.shtml?stn=8772440%20Freeport,%20TX&type=Tide%20Data), accessed May 16, 2007.~~

Source 1 Mareogram Summary:

Location	Region	Travel Time (hr-min)	Peak Height(cm)	Initial Motion	Period (hr-min)
Brownsville_TX	Gulf	6 hours 22min	4	depression	2 hours 3 min
Corpus Christi_TX	Gulf	6 hours 45 min	4	depression	1 hour 18 min
Galveston_TX	Gulf	8 hours 2 min	6	depression	1 hour 58 min
High Island_TX	Gulf	8 hours 30 min	3	depression	1 hour 57 min
Eugene Island_LA	Gulf	8 hours 10 min	3	depression	1 hour 56 min
Port Fourchon_LA	Gulf	5 hours 52 min	10	depression	2 hours 3 min
Grand Isle_LA	Gulf	6 hours	12	depression	1 hour 38 min
Waveland_MS	Gulf	10 hours 36 min	1	depression	
Biloxi_MS	Gulf	8 hours 28 min	5	depression	2 hours 5 min
MS_AL Border	Gulf	9 hours 35 min	3	depression	2 hours 2 min
Destin_FL	Gulf	5 hours 38 min	7	depression	1 hour 55 min
Suwanee_FL	Gulf	8 hours 37 min	3	depression	2 hours 2 min
Panama Beach_FL	Gulf	5 hours 47 min	5	depression	1 hour 54 min
Panama City_FL	Gulf	6 hours 20 min	11	depression	2 hours 2 min
Clearwater Bc_FL	Gulf	6 hours 58 min	8	depression	1 hour 6 min
St Petersburg_FL	Gulf	7 hours 48 min	5	depression	2 hours 56 min
Tampa_FL	Gulf	8 hours 28 min	5	depression	2 hours 28 min
Port Manatee_FL	Gulf	7 hours 28 min	5	depression	1 hour 28 min
Bonita_FL	Gulf	7 hours 37 min	25	depression	1 hour 50 min
Naples_FL	Gulf	7 hours 28 min	23	depression	1 hour
Virginia Key_FL	Atlantic	2 hours 57 min	15	elevation	49 min
Ocean Reef_FL	Atlantic	3 hours 13 min	28	elevation	1 hour 40 min
Jupiter_FL	Atlantic	2 hours 47 min	54	elevation	1 hour 2 min
Flagler_FL	Atlantic	4 hours 18 min	117	elevation	1 hour 10 min
Vaca Key_FL	Atlantic	4 hours	13	elevation	1 hour 11 min
St Simons_GA	Atlantic	5 hours 30 min	40	elevation	1 hour 13 min
Altamaha_GA	Atlantic	5 hours 33 min	47	elevation	1 hour 15 min
So Santee_SC	Atlantic	4 hours 32 min	77	elevation	1 hour 22 min
Springmaid_SC	Atlantic	4 hours 57 min	129	elevation	1 hour 8 min
Charleston_SC	Atlantic	4 hours 57 min	49	elevation	1 hour 15 min
Surf City_NC	Atlantic	4 hours 23 min	112	elevation	1 hour 8 min
Beaufort_NC	Atlantic	3 hours 38 min	147	elevation	45 min
Oregon Inlet_NC	Atlantic	3 hours 45 min	38	elevation	42 min
Duck_NC	Atlantic	3 hours 57 min	140	elevation	drained
Currituck_NC	Atlantic	4 hours 15 min	102	elevation	36 min
Chesapeake B_VA	Atlantic	7 hours 12 min	6	elevation	46 min
Annapolis_MD	Atlantic	10 hours 28 min	3	elevation	~2 hours
Cape Henlopen_DE	Atlantic	4 hours 52 min	64	elevation	42 min
Cape May_NJ	Atlantic	5 hours	68	elevation	45 min
Atlantic City_NJ	Atlantic	4 hours 45 min	155	elevation	45 min
Montauk_NY	Atlantic	4 hours 48 min	68	elevation	16 min
Bar Harbor_ME	Atlantic	5 hours 33 min	71	elevation	6 min
D41424 (32.4N, 73W)	Atlantic	1 hour 52 min	35	elevation	
D41420 (23.3N, 67.6W)	Atlantic	32 min	131	elevation	
D41421 (23.4N, 63.9W)	Atlantic	31 min	175	elevation	
D7-2 (38.6N, 68 W)	Atlantic	2 hours 10 min	78	elevation	
D42407 (23.4N, 63.9W)	Caribbean	10 min	-61	depression	
D8-1 (25.4N, 86.8W)	Gulf	3 hours 27 min	-2	depression	
Bermuda	Atlantic	1 hour 57 min	511	elevation	12 min
Limetre StCroix	Caribbean	1 min	240	depression	15 min
Punta Guayanilla	Caribbean	0 min	173	elevation	21 min

Figure 2.4S.6-23 ~~Map of Predicted Runup Elevations for a Simulated “Worst Case” M<sub>w</sub> 9.0 Earthquake in the Puerto Rico Trench~~

Source: Reference 2.4S.6-1, p. 309

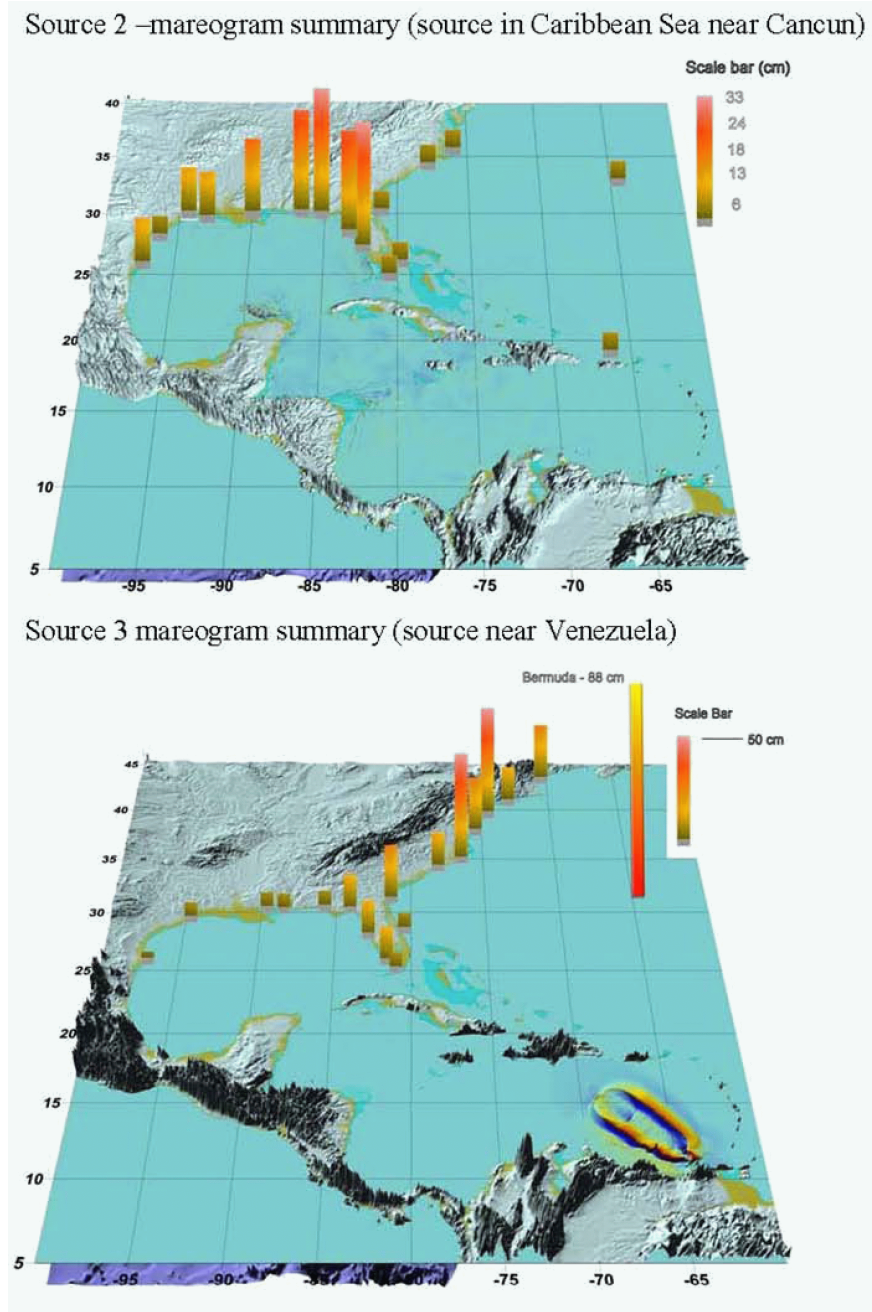


**Figure 2.4S.6-24 Map of Predicted Runup Elevations for a Simulated “Worst Case”  $M_w$  8.2 earthquake (Source 2) along the North Caribbean Plate Boundary and a  $M_w$  9.0 in the North Panama Deformed Belt (Source 3)**

Source: Reference 2.4S.6-1, p. 309 Reference 2.4S.6-1, p. 310

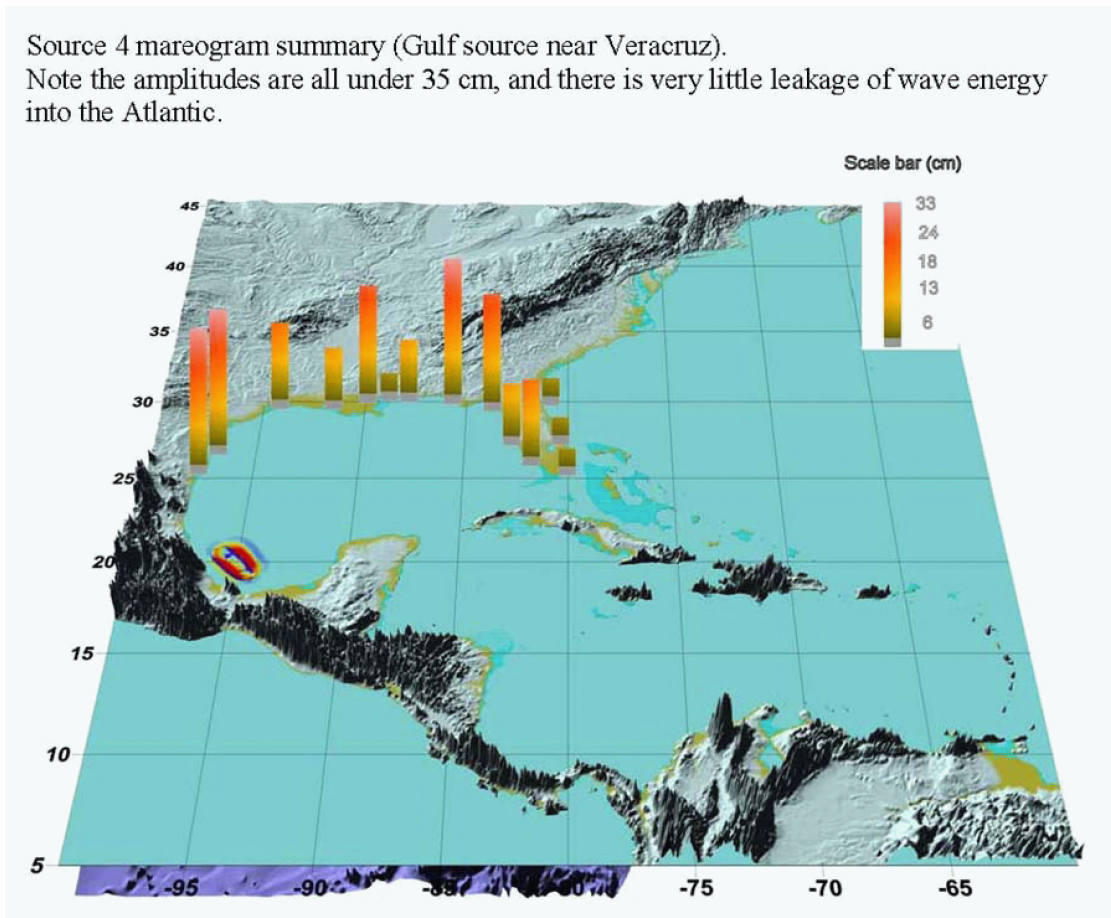


**Figure 2.4S.6-25 ~~Map of Predicted Runup Elevations for a Hypothetical "Worst Case" Earthquake near Veracruz, Mexico~~**

Source: Reference 2.4S.6-1, p. 311

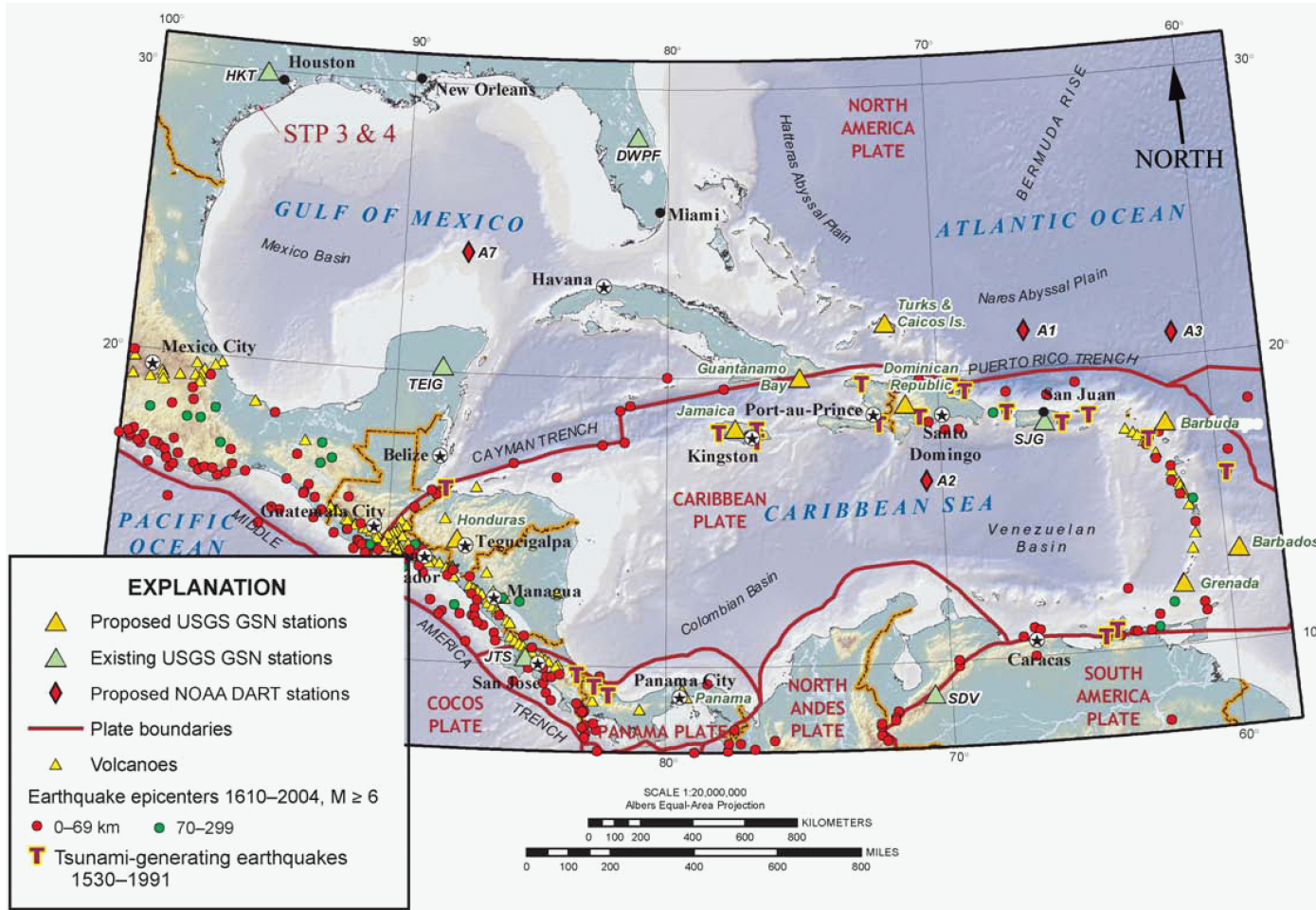


Figure 2.4S.6-26 **Regional Map of Plate Boundaries and Tsunami-Generating Earthquakes from 1530–1991 in the Caribbean Sea (modified from Reference 2.4S.6-9)**

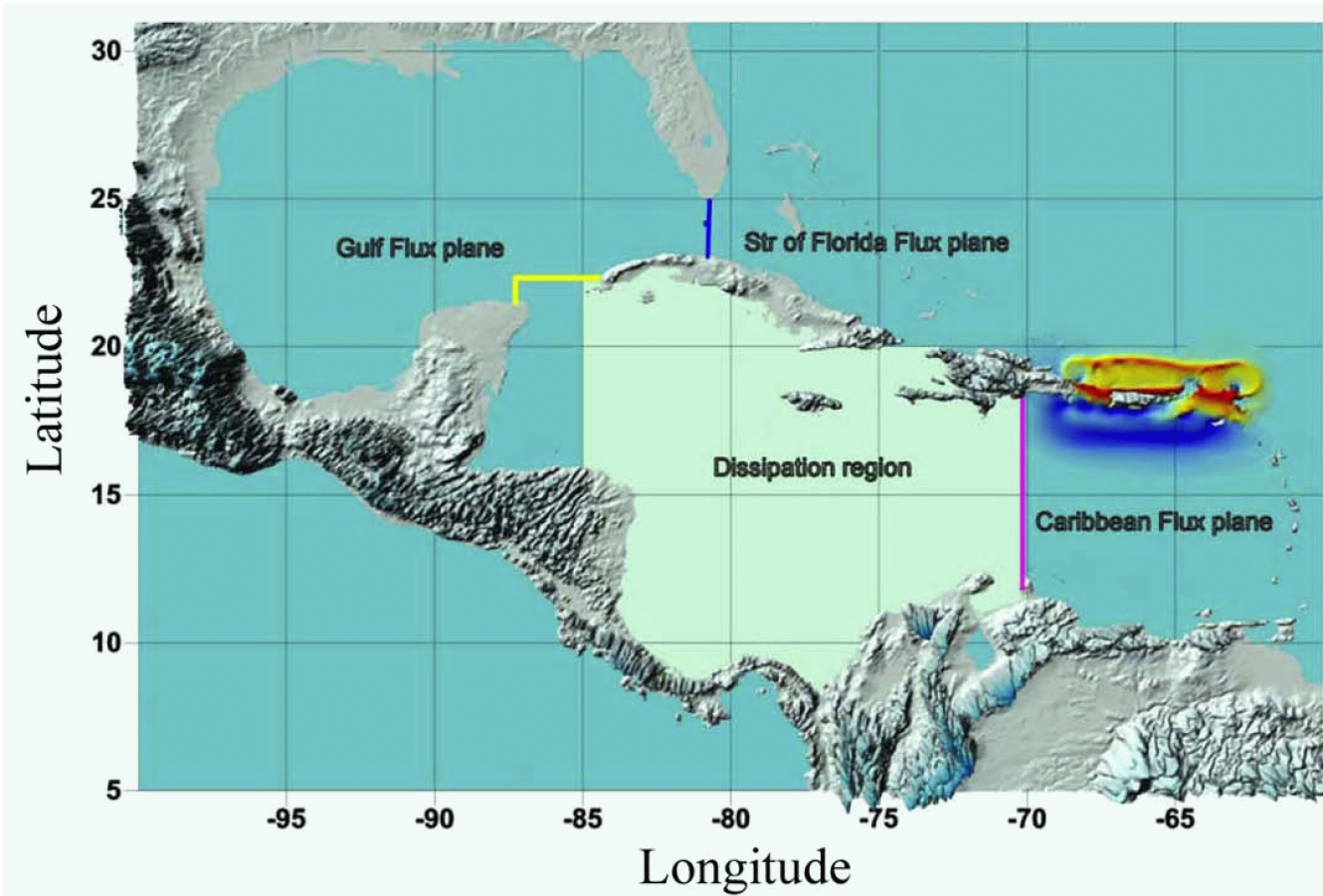


Figure 2.4S.6-27 **Regional Map of the Straits of Florida, Gulf Flux, and Caribbean Flux Planes with Respect to Energy Dissipation in the Caribbean Sea**

Source: Reference 2.4S.6-1, p. 308

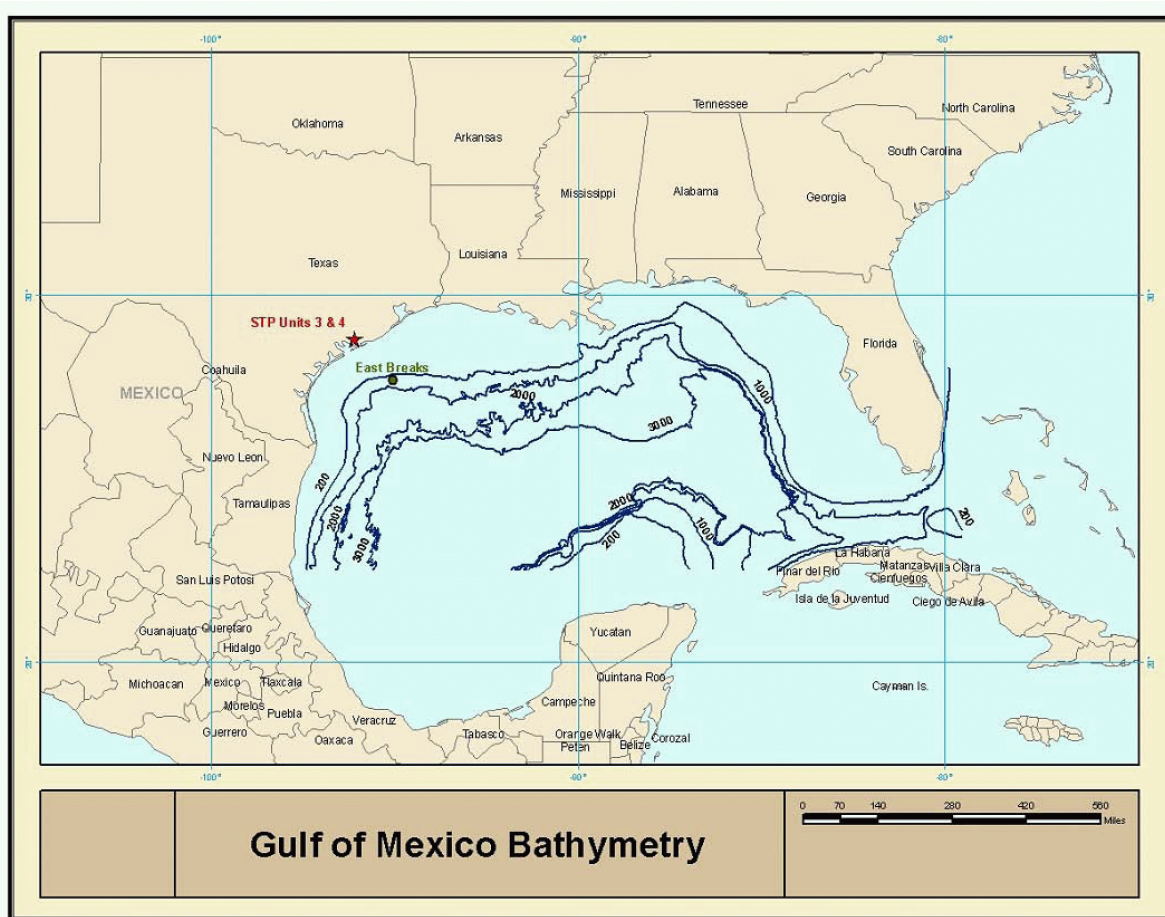


Figure 2.4S.6-28 ~~Gulf of Mexico Bathymetry and Location of the East Breaks Slump Area. The Contour Labels Represent Depths (feet) in the Gulf of Mexico~~

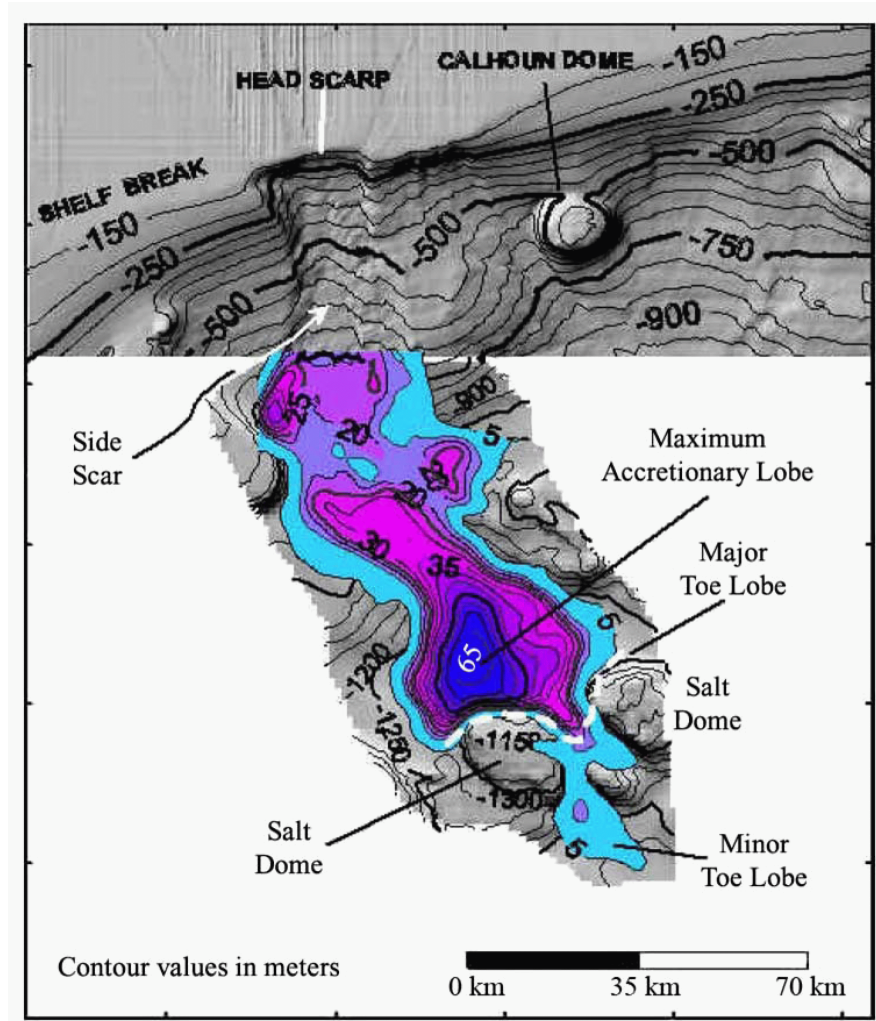


Figure 2.4S.6-29 ~~Map and Dimensions of the East Breaks Slump Location from the Northwestern Gulf of Mexico~~

Source: Reference 2.4S.6-5, p. 5